Lymphomyeloid Contribution of an Immune-Restricted Progenitor Emerging Prior to Definitive Hematopoietic Stem Cells

Charlotta Böiers, Joana Carrelha, Joanna c.A. Green, Emanuele Azzoni, Petter s. Woll, Adam j. Mead, Anne Hultquist, Gemma Swiers, Elisa gomez Perdiguero, Iain c. Macaulay, et al.

Please cite this article in press as: Böiers et al., Lymphomyeloid Contribution of an Immune-Restricted Progenitor Emerging Prior to Definitive Hematopoietic Stem Cells, Cell Stem Cell (2013), http://dx.doi.org/10.1016/j.stem.2013.08.012

Cell Stem Cell
Article

Lymphomyeloid Contribution of an Immune-Restricted Progenitor Emerging Prior to Definitive Hematopoietic Stem Cells

Charlotta Böiers,[1,2] Joana Carrelha,[3] Michael Lutteropp,[3] Sidinh Luc,[3] Joanna C.A. Green,[3] Emanuele Azzoni,[4] Petter S. Woll,[3] Adam J. Mead,[3] Anne Hultquist,[1] Gemma Swiers,[4] Elisa Gomez Perdiguero,[5] Iain C. Macaulay,[3] Luca Melchiori,[3] Tiago C. Luis,[3] Shabnam Kharazi,[1] Tiphaine Bouriez-Jones,[3] Qiaolin Deng,[6] Annica Pontén,[7] Deborah Atkinson,[3] Christina T. Jensen,[3] Ewa Sitnicka,[1] Frederic Geissmann,[5] Isabelle Godin,[8] Rickard Sandberg,[6] Marella F.T.R. de Bruijn,[4] and Sten Eirik W. Jacobsen[3,4,9,*]

[1]Haematopoietic Stem Cell Laboratory, Lund Stem Cell Center, Lund University, 221 84 Lund, Sweden
[2]Molecular Medicine and Gene Therapy, Lund Stem Cell Center, Lund University, 221 84 Lund, Sweden
[3]Haematopoietic Stem Cell Laboratory, Weatherall Institute of Molecular Medicine, John Radcliffe Hospital, University of Oxford, Headington, Oxford OX3 9DS, UK
[4]MRC Molecular Haematology Unit, Weatherall Institute of Molecular Medicine, John Radcliffe Hospital, University of Oxford, Headington, Oxford OX3 9DS, UK
[5]Center for Molecular and Cellular Biology of Inflammation, Division of Immunology Infection & Inflammatory Diseases, King's College London, London SE1 1UL, UK
[6]Department of Cell and Molecular Biology, Karolinska Institutet and Ludwig Institute for Cancer Research, 171 77 Stockholm, Sweden
[7]Cardiovascular group, Lund Stem Cell Center, Lund University, 221 84 Lund, Sweden
[8]Institut National de la Santé et de la Recherche Médicale, INSERM 1009, Université Paris-Sud, Orsay, 94805 Villejuif, France
[9]Department of Cell and Molecular Biology, Wallenberg Institute for Regenerative Medicine and Department of Medicine, Center for Hematology and Regenerative Medicine, Karolinska Institutet, 171 77 Stockholm, Sweden
*Correspondence: sten.jacobsen@imm.ox.ac.uk
http://dx.doi.org/10.1016/j.stem.2013.08.012

SUMMARY

In jawed vertebrates, development of an adaptive immune-system is essential for protection of the born organism against otherwise life-threatening pathogens. Myeloid cells of the innate immune system are formed early in development, whereas lymphopoiesis has been suggested to initiate much later, following emergence of definitive hematopoietic stem cells (HSCs). Herein, we demonstrate that the embryonic lymphoid commitment process initiates earlier than previously appreciated, prior to emergence of definitive HSCs, through establishment of a previously unrecognized entirely immune-restricted and lymphoid-primed progenitor. Notably, this immune-restricted progenitor appears to first emerge in the yolk sac and contributes physiologically to the establishment of lymphoid and some myeloid components of the immune-system, establishing the lymphomyeloid lineage restriction process as an early and physiologically important lineage-commitment step in mammalian hematopoiesis.

INTRODUCTION

The mammalian hematopoietic system is considered the paradigmatic and best-understood model for how multilineage diversity is achieved by stepwise lineage restriction of a multipotent stem cell (Orkin and Zon, 2008a). Although multipotent hematopoietic stem cells (HSCs) possessing all blood-lineage potentials have been unequivocally established to reside at the top of the hematopoietic hierarchy (Osawa et al., 1996), the exact roadmap for hematopoietic lineage restriction remains disputed, in particular with regard to the first lineage-restriction steps of HSCs (Orkin and Zon, 2008a; Schlenner and Rodewald, 2010; Ye and Graf, 2007). The classical hematopoietic hierarchy still prevailing in textbooks predicts that the first lineage-restriction decision made by adult HSCs results in strictly separated pathways for the lymphoid and myeloerythroid lineages (Orkin and Zon, 2008b; Seita and Weissman, 2010) as supported by the identification of common lymphoid (Kondo et al., 1997) and common myeloid (Akashi et al., 2000; Arinobu et al., 2007) progenitors (CLPs and CMPs, respectively).

However, earlier in vitro findings demonstrating that clonal lineage outputs of heterogeneous fetal hematopoietic progenitors excluded combined B and T cell generation in the absence of myeloid cells, challenged the classical hematopoietic hierarchy, and led to the proposal that the first lineage decisions of HSCs might rather result in a separation into a CMP and a lymphomyeloid progenitor pathway (Katsura and Kawamoto, 2001), a hypothesis supported by additional studies (Cumano et al., 1992; Lacaud et al., 1998). More recently, lymphoid-primed multipotent progenitors (LMPPs) were prospectively isolated and shown at the single-cell level to possess combined granulocyte-macrophage (GM) and B and T lymphocyte potential but little or no megakaryocyte-erythroid (MkE) potential (Adolfsson et al., 2005; Månsson et al., 2007), providing direct evidence for the existence of a lymphomyeloid-restricted pathway in mammalian hematopoiesis. However, the revised

Please cite this article in press as: Böiers et al., Lymphomyeloid Contribution of an Immune-Restricted Progenitor Emerging Prior to Definitive Hematopoietic Stem Cells, Cell Stem Cell (2013), http://dx.doi.org/10.1016/j.stem.2013.08.012

hematopoietic hierarchy has been challenged by studies implying that LMPPs possess considerable MkE potential in vivo (Boyer et al., 2011; Forsberg et al., 2006). Thus, whether the first lineage fate decision of multipotent stem-progenitor cells results in establishment of completely separated pathways of the myeloid and lymphoid components of the immune system or a common lymphomyeloid immune pathway remains unresolved (Boyer et al., 2012; Orkin and Zon, 2008a; Schlenner and Rodewald, 2010; Seita and Weissman, 2010; Ye and Graf, 2007). Moreover, the in vivo physiological relevance of the lymphomyeloid pathway has been challenged based on in vivo fate mapping studies concluding that adult lymphomyeloid-restricted progenitors contribute almost exclusively to lymphopoiesis and not myelopoiesis (Boyer et al., 2011; Schlenner et al., 2010; Welner et al., 2009).

Lineage-fate decisions of multipotent stem and progenitor cells take place for the first time during early embryonic development. Blood cells appear in the mouse embryo at embryonic day (E) 7 in the yolk sac (YS). This first wave of primitive hematopoiesis is myeloerythroid-restricted and transient (Medvinsky et al., 2011). In addition, resident tissue macrophages, such as brain microglia, liver Kupffer cells, and epidermal Langerhans cells, develop between E8.5 and E9.5 independently of definitive HSCs (Schulz et al., 2012). The first definitive multipotent HSCs, defined as cells capable of long-term repopulation of all myeloerythroid and lymphoid lineages in adult recipient mice are not found until after E10.5 (Medvinsky and Dzierzak, 1996). These HSCs, first generated in the aorta-gonad-mesonephros (AGM) region, subsequently at E11 seed the fetal liver (FL), the main fetal hematopoietic site (Kumaravelu et al., 2002; Medvinsky and Dzierzak, 1996). Because the first lymphoid-restricted embryonic progenitors have been identified after definitive HSCs seed the FL (Douagi et al., 2002), it has been assumed that lymphoid lineage restriction does not initiate before the FL is seeded by definitive HSCs. However, there are several findings compatible with lymphoid lineage commitment potentially initiating earlier. Progenitors possessing all myeloerythroid and lymphoid lineage potentials have been identified before emergence of definitive HSCs and FL hematopoiesis (Kieusseian et al., 2012; Rybtsov et al., 2011; Yoshimoto et al., 2012) and at E10.5–E11, low-level expression of interleukin-7 receptor alpha (IL7Rα) and the recombination activating gene 1 (*Rag1*), regulators of early lymphoid development, have been described in the embryo (Kawamoto et al., 2000; Yokota et al., 2006) Although the identity of these early IL7Rα and *Rag1*-expressing cells has not been investigated in detail, they could potentially reflect multilineage transcriptional-primed multipotent progenitors (Hu et al., 1997; Månsson et al., 2007). However, the earliest IL7Rα-expressing progenitors have rather been suggested to be fully B or T lymphocyte-restricted and to lack myeloid lineage potential (Kawamoto et al., 2000), coinciding with or even preceding evidence of lymphomyeloid lineage restriction, suggesting that B and T lymphoid lineage restriction might occur independently of a lymphomyeloid lineage restriction step.

Herein we prospectively identified an IL7Rα-expressing lymphomyeloid-restricted embryonic progenitor as early as E11.5 that sustains combined lymphoid and GM transcriptional lineage priming and potential at the single-cell level but lacks MkE potential. We tracked this lymphomyeloid progenitor back to E9.5 YS, preceding both hematopoietic colonization of the FL and the establishment of definitive HSCs. Through in vivo fate mapping, we confirmed the inability of *Rag1*-expressing early embryonic progenitors to significantly contribute to the MkE lineage while unequivocally and robustly contributing to the myeloid innate, as well as lymphoid adaptive, immune systems of the mammalian embryo. These findings identify the developmentally earliest immune-restricted progenitor and establish the lymphomyeloid restriction as a physiologically important lineage-commitment step in embryonic mammalian hematopoiesis, preceding the emergence of definitive HSCs.

RESULTS

Interleukin-7 Receptor Expression Defines Immune-Restricted Embryonic Progenitors with Combined Lymphoid and Granulocyte-Macrophage Lineage Potentials

Expression of IL7Rα has been suggested to be restricted to lymphoid progenitors. We investigated IL7Rα expression in FL at E11.5 and in agreement with previous findings (Kawamoto et al., 2000) we found IL7Rα$^+$ cells coexpressing the pan-hematopoietic marker CD45 and the progenitor cell receptor c-Kit (Kit) but negative for mature lineage markers (Lin$^-$) (Figure 1A). A large fraction of Lin$^-$Kit$^+$IL7Rα$^+$ cells also expressed the myeloid colony-stimulating factor 1 receptor (Csf1r) and the thrombopoietin receptor (ThpoR) (Figure 1A), also expressed by HSCs (Solar et al., 1998). Most IL7Rα$^+$ cells (>70%) coexpressed c-fms-like tyrosine kinase 3 receptor (Flt3) (0.20% of FL cells; Figure 1B), highly expressed on early lymphomyeloid progenitors in adult bone marrow (Adolfsson et al., 2005). Single-cell assays demonstrated that Lin$^-$Kit$^+$Flt3$^+$IL7Rα$^+$ E11.5 FL cells possess considerable GM potential with as many as 43% of single cells forming GM clones, whereas virtually no cells (<1%) possessed Mk or E potential (Figures 1C–1F). Single Lin$^-$Kit$^+$Flt3$^+$IL7Rα$^+$ cells generated 31% and 35% of B and T cell progeny, respectively (Figures 1G and 1H). In vitro cytokine response experiments with the ligands for Flt3 and IL7Rα demonstrated that Flt3 and IL7Rα are expressed at functionally relevant levels on Lin$^-$Kit$^+$Flt3$^+$IL7Rα$^+$ progenitors (see Figure S1A available online). However, in contrast to later emerging B and T lymphoid-restricted progenitors critically dependent on Flt3 and IL7Rα signaling (Sitnicka et al., 2003), investigation of embryos genetically deleted for expression of both Flt3 ligand and the common gamma chain of the IL7R demonstrated that E11.5 Lin$^-$Kit$^+$Flt3$^+$IL7Rα$^+$ progenitors emerge independently of Flt3 and IL7R signaling (Figures S1B and S1C).

Investigation of single Lin$^-$Kit$^+$Flt3$^+$IL7Rα$^+$ E11.5 FL cells demonstrated that more than 70% coexpressed lymphoid (*Il7r*, *Rag1*, and *sIgh)* and GM (*Csf3r* [*Gcsfr*] and *Mpo*), but not the MkE (*Vwf*, *Epor*, and *Gata1*) transcripts typically expressed by multipotent progenitors with MkE potential (Figures 2A and 2B)(Månsson et al., 2007). When compared to Lin$^-$Kit$^+$Flt3$^-$IL7Rα$^-$ cells, the downregulation of MkE-affiliated and upregulation of lymphoid genes expressed prior to B and T cell commitment was further verified through single-cell quantitative gene expression analysis (Figure 2C). Notably,

Please cite this article in press as: Böiers et al., Lymphomyeloid Contribution of an Immune-Restricted Progenitor Emerging Prior to Definitive Hematopoietic Stem Cells, Cell Stem Cell (2013), http://dx.doi.org/10.1016/j.stem.2013.08.012

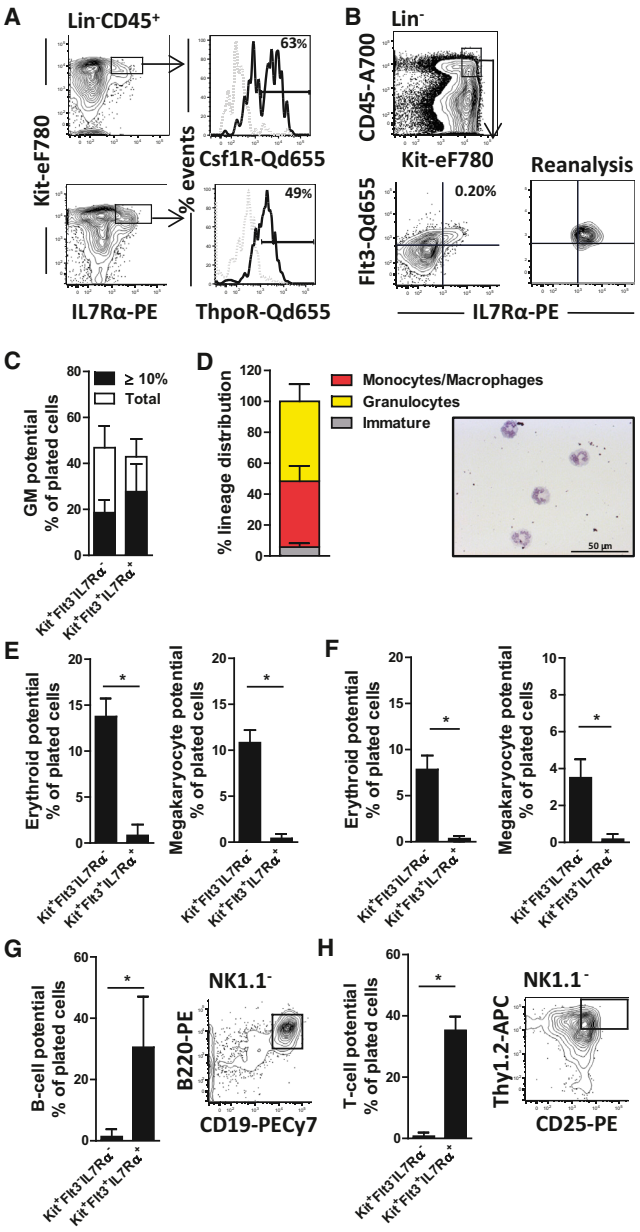

Figure 1. Interleukin-7-Receptor Expressing Early Fetal Liver Progenitors Have Lymphomyeloid Lineage Potentials

(A) Coexpression of cell-surface IL7Rα, Csf1R (upper panel) and ThpoR (lower panel) in E11.5 FL Lin$^-$Kit$^+$ progenitors. Viable cells were gated Lin$^-$CD45$^+$. Further gating is indicated in the figure. Grey lines represent negative controls. Mean percentages of Lin$^-$CD45$^+$Kit$^+$IL7Rα$^+$ cells coexpressing Csf1R or ThpoR, respectively, are shown (three experiments).

(B) Lin$^-$Kit$^+$Flt3$^+$IL7Rα$^+$ E11.5 FL cell purification by FACS (purity reanalysis right panel). Mean percentage of total FL cells (>3 experiments) is shown.

(C) GM lineage potential in liquid culture of single Lin$^-$Kit$^+$Flt3$^-$IL7Rα$^-$ and Lin$^-$Kit$^+$Flt3$^+$IL7Rα$^+$ E11.5 FL cells (white bars represent total cloning; black bars represent clones covering ≥ 10% of well; >350 cells per population). Mean ± SD.

(D) Bulk-sorted Lin$^-$Kit$^+$Flt3$^+$IL7Rα$^+$ E11.5 FL cells were cultured under myeloid conditions and evaluated morphologically. Mean ± SD (three biological replicates). Right panel shows representative granulocytes.

(E) Erythroid (left panel) and megakaryocyte (right panel) lineage potential of single Lin$^-$Kit$^+$Flt3$^-$IL7Rα$^-$ and Lin$^-$Kit$^+$Flt3$^+$IL7Rα$^+$ E11.5 FL cells in liquid culture. Mean percentages ± SD (≥450 cells per assay).

this single-cell analysis demonstrated that every Lin$^-$Kit$^+$Flt3$^+$IL7Rα$^+$ progenitor cell expressing these lymphoid genes coexpressed myeloid lineage genes, whereas none of them expressed signature genes of the earliest B (*Pax5*) and T (*Ptcra*) cell restricted progenitors.

Clones derived from single Lin$^-$Kit$^+$Flt3$^+$IL7Rα$^+$ E11.5 FL cells were analyzed for the combined potential for generation of GM, B, and T cells (Figures 2D and 2E). Of the single cell-derived clones that gave a lineage readout, as many as 45% produced mature cells of all three GM, B, and T cell lineages (GM/B/T; Figures 2F and 2G). Natural killer (NK) cells, a third lymphoid lineage and part of the innate immune system, were generated in the majority of the single cell-derived GM/B/T clones (Figure 2H). Virtually no erythroid cells were produced even upon inclusion of erythroid-promoting cytokines (Figure 2I), which stimulated erythropoiesis from the more heterogeneous Lin$^-$Kit$^+$Flt3$^-$IL7Rα$^-$ progenitors (Figures S2A and S2B).

Paired immunoglobulin like receptor (PIR) expression has been shown to separate T and B cell progenitors later in embryonic development. Specifically, in E13.5, FL T cell restricted progenitors were found to coexpress IL7Rα and PIR, whereas B cell progenitors were IL7Rα$^+$PIR$^-$ (Masuda et al., 2005). We found that only a small fraction (11%) of E11.5 FL Lin$^-$Kit$^+$Flt3$^+$IL7Rα$^+$ progenitors expressed cell surface PIR (Figure 2J). The PIR expression was confirmed by quantitative PCR and shown to coincide with upregulation of other early lymphoid transcripts, whereas both PIR$^+$ and PIR$^-$ Lin$^-$Kit$^+$Flt3$^+$IL7Rα$^+$ cells expressed myeloid genes (Figure 2K). In agreement with representing the E11.5 FL lymphomyeloid-restricted progenitors with combined GM, B, and T cell potential, Lin$^-$Kit$^+$Flt3$^+$IL7Rα$^+$PIR$^-$ cells showed robust readout of all three lineage potentials, whereas the small fraction of Lin$^-$Kit$^+$Flt3$^+$IL7Rα$^+$PIR$^+$ cells showed reduced T and undetectable B cell potential (Figure 2L). Thus, at the time of its first seeding by definitive HSCs, the FL contains Lin$^-$Kit$^+$Flt3$^+$IL7Rα$^+$ progenitors with combined lymphomyeloid, but no MkE transcriptional priming or potential.

Emergence of Immune-Restricted Progenitors Prior to Definitive HSCs

A large number of Lin$^-$Kit$^+$Flt3$^+$IL7Rα$^+$ immune-restricted progenitors (1,200 ± 200 cells/FL) were already present by E11.5. In contrast, we did not detect any long-term multilineage reconstitution activity in E10.5 or E11.5 FL (whether transplanted intravenously or directly into the bones), whereas considerable HSC activity was found in E12.5 FL (Figure 3A; Figures S3A–S3D). These findings are in agreement with previous studies, which suggest that there is at most only one definitive HSC in the FL at E11.5 (Kumaravelu et al., 2002). To enhance the possibility

(F) Erythroid (left panel) and megakaryocyte (right panel) potential of Lin$^-$Kit$^+$Flt3$^+$IL7Rα$^+$ E11.5 FL cells in semisolid medium. Mean percentages ± SD (600 cells, 3 experiments).

(G) B cell (NK1.1$^-$CD19$^+$B220$^+$) and (H) T cell (NK1.1$^-$CD25$^+$Thy1.2^{hi} and/or NK1.1$^-$CD4$^+$CD8$^+$) potential of single Lin$^-$Kit$^+$Flt3$^-$IL7Rα$^-$ and Lin$^-$Kit$^+$Flt3$^+$IL7Rα$^+$ E11.5 FL cells in Op9 and Op9DL1 coculture, respectively. Representative FACS plots. Mean percentages ± SD (≥90 cells per assay), *$p \leq 0.05$.

See also Figure S1.

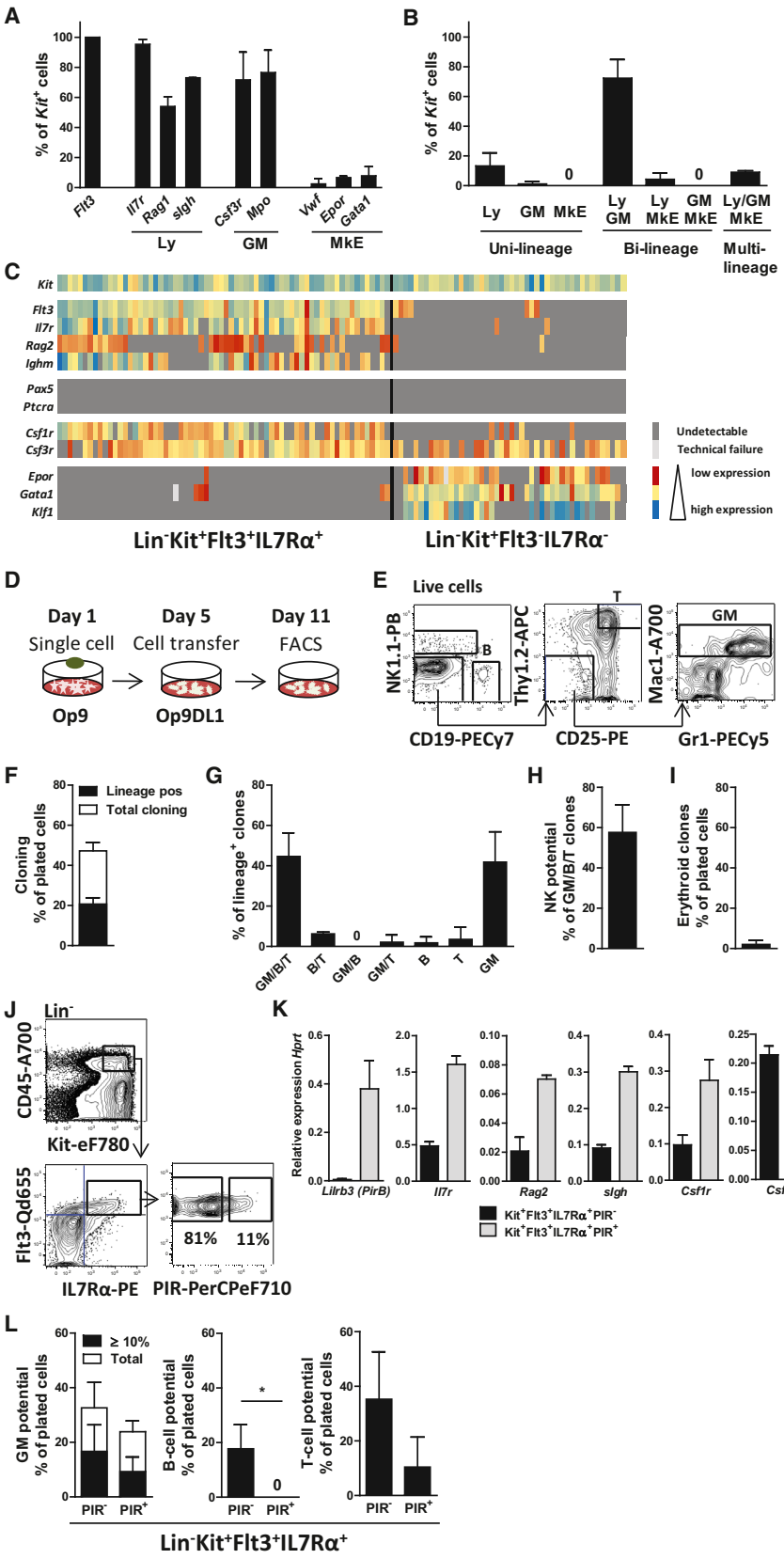

Figure 2. Combined GM and Lymphoid Transcriptional Priming and Lineage Potentials of Single IL7Rα+ E11.5 Fetal Liver Progenitors

(A) Single-cell RT-PCR analysis of Lin⁻Kit⁺Flt3⁺IL7Rα⁺ E11.5 FL cells and (B) combined lineage transcriptional priming patterns based on (A). Mean percentages ± SD of total *Kit*⁺ cells (>93%; ≥130 cells).

(C) Quantitative gene-expression analysis of single Lin⁻Kit⁺Flt3⁺IL7Rα⁺ and Lin⁻Kit⁺Flt3⁻IL7Rα⁻ E11.5 progenitors. Expression of early lymphoid (*Flt3*, *Il7r*, *Rag2*, *Ighm*), B cell-specific (*Pax5*), T cell-specific (*Ptcra*), myeloid (*Csf1r*, *Csf3r*), and MkE (*Epor*, *Gata1*, *Klf1*) related genes were determined as Δ Ct values and normalized to the mean of *Gapdh* and *Hprt*. Each column represents a single cell (≥45 cells per population).

(D) Experimental strategy for establishing combined lineage potentials of Lin⁻Kit⁺Flt3⁺IL7Rα⁺ E11.5 FL cells. Single cells were deposited directly into wells with Op9 stroma cells. After 5 days of culture, clones were transferred to Op9DL1 stroma cells. Clones were analyzed for lineages after 11 days of culture.

(E) Representative FACS profile of Lin⁻Kit⁺Flt3⁺IL7Rα⁺ E11.5 FL single-cell-derived GM/B/T clone. A clone was scored positive for B cells if containing NK1.1⁻CD19⁺ cells; T cells if NK1.1⁻CD19⁻CD25⁺Thy1.2^{hi} cells and GM cells if containing NK1.1⁻CD19⁻CD25⁻Thy1.2⁻Mac1⁺Gr1$^{-/+}$ cells.

(F) Cloning frequency (white bar; black bar represents clones assigned to the GM, B, and/or T lineage) and (G) lineage (GM/B/T) composition of lineage-positive clones derived from single Lin⁻Kit⁺Flt3⁺IL7Rα⁺ E11.5 FL cells and (H) frequency of combined GM/B/T clones also containing NK (NK1.1⁺CD19⁻CD25⁻Thy1.2⁻) cells. Data in (F)–(H) are mean percentages ± SD (≥230 cells investigated).

(I) Frequency of Lin⁻Kit⁺Flt3⁺IL7Rα⁺ E11.5 FL progenitors with erythroid potential (clones with Ter119⁺CD71⁺ cells and/or positive by morphology) on Op9 stroma under conditions promoting erythroid development. Mean percentage ± SD of plated cells (150 cells investigated, 3 experiments).

(J) Lin⁻Kit⁺Flt3⁺IL7Rα⁺ E11.5 FL progenitors were fractionated based on expression of PIR. Mean percentages within Lin⁻Kit⁺Flt3⁺IL7Rα⁺ compartment (four experiments).

(K) Quantitative gene expression analysis of lymphoid and myeloid transcripts in Lin⁻Kit⁺Flt3⁺IL7Rα⁺PIR⁻ and PIR⁺ cells. Mean expression ± SD normalized to *Hprt* (2 biological replicates, 25 cells per population).

(L) Lineage potentials of single Lin⁻Kit⁺Flt3⁺IL7Rα⁺PIR⁻ and PIR⁺ cells. GM potential (left panel) (white bars represent total cloning; black bars represent clones covering ≥10% of well), B cell potential (middle panel), and T cell potential (right panel). Mean percentages ± SD; two to three experiments, *p ≤ 0.05.

See also Figure S2.

to identify rare lymphoid-primed progenitors in the early FL, and because expression of Flt3 and *Rag1*-GFP highly overlap in Lin$^-$Kit$^+$Flt3$^+$IL7Rα^+ E11.5 progenitors (Figure 3B), we used a *Rag1*-GFP reporter to identify a distinct population of Lin$^-$Kit$^+$*Rag1*GFP$^+$IL7Rα^+ E10.5 FL progenitors (Figure 3C), which possessed GM, B, and T cell, but no MkE potential, as in the E11.5 FL (Figures 3D–3G; Figure S3E), establishing that immune-restricted progenitors are present in the FL already prior to and independently of definitive HSCs.

We next explored how early Lin$^-$Kit$^+$*Rag1*GFP$^+$IL7Rα^+ lymphomyeloid-primed progenitors emerge in the embryo. In whole E8.5 concepti, virtually no *Rag1*GFP$^+$IL7Rα^+-positive cells were found, neither in the CD45$^-$ nor in the small CD45$^+$ fraction (Figure 3H). Because the first hematopoietic cells to colonize the FL at E10 might come from the YS, we analyzed YS at E9.5 and observed a small but distinct Lin$^-$Kit$^+$*Rag1*GFP$^+$IL7Rα^+ cell population (30 ± 4 cells/YS; Figure 3I). Notably, whereas most hematopoietic cells at E9.5 have yet to upregulate expression of the pan-hematopoietic marker CD45, virtually all Lin$^-$Kit$^+$*Rag1*GFP$^+$IL7Rα^+ cells were CD45$^+$ although most also expressed CD41, and a small fraction the endothelial marker VE-Cadherin (Figure 3J). The placenta and the para-aortic-splanchnopleura (PAS, to become the AGM) region from E9.5 embryos were also investigated, but no *Rag1*GFP$^+$IL7Rα^+ cells were detected above background level (Figure 3I).

Almost 80% of the rare purified E9.5 YS Lin$^-$Kit$^+$*Rag1*GFP$^+$IL7Rα^+ cells expressed combined lymphoid GM but no MkE transcriptional priming at the single-cell level (Figures 3K and 3L), similar to E11.5 FL Lin$^-$Kit$^+$Flt3$^+$IL7Rα^+ cells (Figures 2A–2B), demonstrating that lymphomyeloid-primed progenitors emerge as early as E9.5.

To further investigate the embryonic site of origin of the lymphoid-primed immune-restricted progenitors, whole-mount imaging of *Rag1*GFP$^+$ embryos was performed. In agreement with the fluorescence-activated cell sorting (FACS) analysis, *Rag1*GFP$^+$ cells coexpressing CD45 and the endothelial marker CD31 were localized in the YS at E9.5 in all embryos investigated (14/14; Figure 3M; Figure S3F), whereas in the PAS region *Rag1*GFP$^+$ cells were rarely observed (Figure 3N). Notably, the majority of *Rag1*GFP$^+$ cells in the YS were predominantly located in close proximity to the primitive vascular plexus, rather than in large vessels (Figures 3M–3N; Figure S3F). In line with these data, we also observed transcriptional expression of *Rag2* and *Il7r* in E9.5 YS but little or no expression in E8.5 embryos or E9.5 PAS (Figure 3O). These data are most compatible with Lin$^-$Kit$^+$*Rag1*GFP$^+$IL7Rα^+ cells originating in E9.5 YS. However, because the connection between the YS and intraembryonic blood vessels occurs already at E8.5, we next dissected the YS and PAS regions from *Rag1*GFP$^+$ embryos before circulation was established ($\leq$6 somite pairs [sp]), short-term cultured the whole explants, and performed whole-mount immunolabeling (Cumano et al., 1996). Strikingly, in six out of ten YS explants, *Rag1*GFP$^+$ cells coexpressing CD45 and CD31 emerged after 48 hr, as did expression of *Il7r* and *sIgh* (Figures 3P and 3Q), whereas at the same time no *Rag1*GFP$^+$ cells were generated by the precirculation PAS explants (seven embryos) (Figure S3G), supporting that *Rag1*GFP$^+$IL7Rα^+ lymphomyeloid-restricted progenitors arise de novo in the YS at E9.5.

Rag1$^+$ Immune-Restricted Progenitors Contribute to Fetal Lymphopoiesis and Myelopoiesis In Vivo

It is important to establish to what degree early lymphoid progenitors with sustained myeloid lineage potential in vitro contribute toward generation of myeloid cells under in vivo physiologically relevant conditions. Recent studies exploring this in adult hematopoiesis have questioned the physiological relevance of the residual myeloid potential of early lymphomyeloid progenitors (Boyer et al., 2011; Schlenner et al., 2010; Welner et al., 2009). Thus, although our in vitro experiments demonstrated that embryonic immune-restricted progenitors sustain lymphoid and GM but little or no MkE lineage potentials, they could not establish the contribution of these *Rag1*-expressing progenitors to different hematopoietic cell lineages during embryonic development. Thus, we applied a *Rag1-Cre* fate mapping in which only cells expressing *Rag1* or their progeny will express a yellow fluorescent protein (YFP). As expected, virtually all B and T cells emerging later in the fetus were positive for YFP in E14.5 FL (Figures 4A–4B) as in adult BM (Figure S4A). Moreover, *Rag1* expressing progenitors did not contribute to the Mk or E lineages, as predicted by our negative in vitro findings and the lack of MkE transcriptional priming (Figure 4A; Figures S4A and S4B). However, in contrast to the adult BM, in which we could confirm that *Rag1* expressing progenitors contribute minimally, if at all, to the GM lineage (Figure S4A), 36% of cells of the GM lineage were YFP$^+$ in E11.5 and 16% in E14.5 FLs (Figures 4A, 4C, and 4D; Figures S4C–S4E). Moreover, while erythroid colony forming cells were YFP$^-$, 20% of granulocyte- and macrophage-containing colonies were YFP$^+$ in E14.5 FLs (Figures 4E and 4F). These fate-mapping studies not only confirm the immune-restricted potentials of Lin$^-$Kit$^+$*Rag1*GFP$^+$IL7Rα^+ progenitors under physiological conditions in the early embryo but they also demonstrate that early embryonic *Rag1*-expressing progenitors contribute extensively to generation of GM and lymphoid cells in the embryo. Interestingly, resident tissue macrophages in the form of microglia, liver Kupffer cells, and epidermal Langerhans cells that develop around E8.5 independently of definitive HSCs (Schulz et al., 2012) were only minimally labeled by YFP (Figure S4F), suggesting that these tissues macrophages emerge independently of Lin$^-$Kit$^+$*Rag1*GFP$^+$IL7Rα^+ lymphomyeloid progenitors, in agreement with an origin prior to the emergence of the herein identified lymphomyeloid-restricted progenitor.

Upregulation of Lymphoid and Downregulation of MkE Lineage Programs in Immune-Restricted Progenitors Prior to Emergence of Definitive HSCs

Genetic experiments have suggested that adult and fetal hematopoiesis is largely regulated through distinct molecular pathways (Yuan et al., 2012). However, whereas the global gene expression profiles of adult HSCs and progenitors have been explored extensively, this has not been feasible with early embryonic progenitors, partly because they have largely yet to be prospectively identified but also because of the scarcity of distinct progenitor cells at these early stages of development. We applied a recently established protocol for global RNA sequencing of small cell numbers (Ramsköld et al., 2012) on purified immune-restricted progenitors in E9.5 YS and E10.5 and E11.5 FLs. We compared expression levels of published

Please cite this article in press as: Böiers et al., Lymphomyeloid Contribution of an Immune-Restricted Progenitor Emerging Prior to Definitive Hematopoietic Stem Cells, Cell Stem Cell (2013), http://dx.doi.org/10.1016/j.stem.2013.08.012

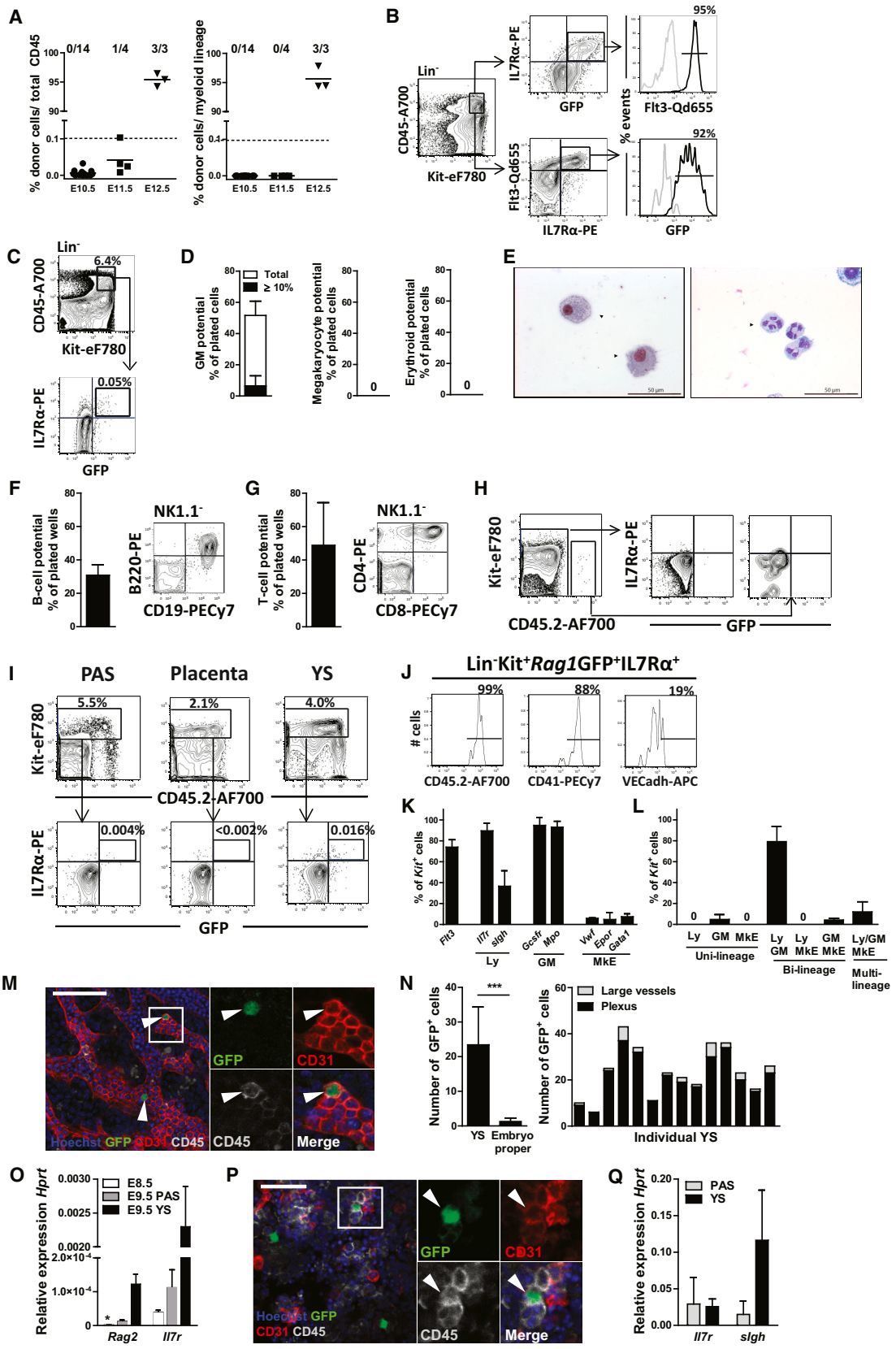

(legend on next page)

lineage-associated genes (Luc et al., 2012) in immune-restricted progenitors (Lin$^-$Kit$^+$*Rag1*GFP$^+$IL7Rα^+ or Lin$^-$Kit$^+$Flt3$^+$IL7Rα^+) with the corresponding Lin$^-$Kit$^+$ progenitors lacking expression of *Rag1*GFP, Flt3, and IL7Rα. This analysis demonstrated a striking upregulation of lymphoid and downregulation of MkE transcripts in E11.5 FL immune-restricted progenitors (Figure 5A), already evident in E10.5 FL and E9.5 YS progenitors (Figure S5A). In agreement with their virtual lack of MkE potential, key MkE regulatory transcripts were markedly downregulated (Figures 5A and 5B), whereas expression of multiple myeloid transcripts was sustained (Figures 5A and 5C). Early lymphoid transcripts were as expected almost undetectable in Lin$^-$Kit$^+$ *Rag1*GFP$^-$IL7Rα^- and Lin$^-$Kit$^+$Flt3$^-$IL7Rα^- progenitors, but markedly upregulated in immune-restricted progenitors at E9.5–E11.5 (Figures 5A and 5D; Figures S5A and S5B). In agreement with our single-cell PCR analysis, early B cell (*Cd79a*, *Ebf1*, *Pax5*, *Vpreb1)* and T cell (*Cd3e*, *Cd8a*, *Ptcra)* restricted transcripts were not expressed in E9.5 YS or E11.5 FL in neither the immune-restricted nor the control progenitors (Figures S5C and S5D), in support of B and T cell-restricted progenitors emerging later in fetal development, or at least not as part of the herein identified Lin$^-$Kit$^+$Rag1GFP$^+$IL7Rα^+ or Lin$^-$Kit$^+$Flt3$^+$ IL7Rα^+ immune-restricted progenitors.

Because the thymic anlage is seeded at E11.5 (Owen and Ritter, 1969), we also investigated the expression of genes implicated in regulation of thymus seeding progenitors (TSPs). Whereas Lin$^-$Kit$^+$*Rag1*GFP$^-$IL7Rα^- and Lin$^-$Kit$^+$Flt3$^-$IL7Rα^- cells expressed little or no *Ccr7* and *Ccr9*, encoding two chemokine receptors critically involved in the migration of embryonic TSPs to the thymus (Liu et al., 2006), both were markedly upregulated in E11.5 FL immune-restricted progenitors and in the case of *Ccr7* already at E9.5 (Figure 5E). Likewise, key regulatory genes in early T cell development such as *Gata3*, *Hes1*, *Notch1*, and *Tcf7* (Rothenberg, 2007) were markedly upregulated in E9.5 and E11.5 immune-restricted progenitors (Figure 5E), compatible with these progenitors possessing TSP potential.

When E9.5–E11.5 immune-restricted progenitors were compared to adult CLPs and LMPPs, investigated lymphoid genes were typically expressed at higher levels than in adult LMPPs (not further separated based on *Rag1*-GFP expression), but in most cases lower than adult CLPs (Figures 5D and 5E; Figure S5B). Selected MkE, GM, lymphoid, and TSP-related transcripts found to be differentially expressed in embryonic immune-restricted cells were further validated with quantitative PCR, confirming the same pattern of gene expression (Figures S6A–S6D). When analyzing the most significantly upregulated transcripts in E9.5 YS Lin$^-$Kit$^+$*Rag1*GFP$^+$IL7Rα^+ (compared to Lin$^-$Kit$^+$*Rag1*GFP$^-$IL7Rα^-) cells and in Lin$^-$Kit$^+$Flt3$^+$IL7Rα^+ E11.5 FL (compared to Lin$^-$Kit$^+$Flt3$^-$IL7Rα^-) cells, 67 transcripts were found to be commonly upregulated at both E9.5 and E11.5 (Figure 6; Tables S1–S3). Notably, the majority of these genes were almost exclusively overrepresented in Gene Ontology Categories related to development or function of the immune system (Figure 6), further supporting the emergence of lymphomyeloid-primed progenitors as an early embryonic commitment step toward establishing a fully competent mammalian immune system.

Figure 3. Emergence of Lymphomyeloid Progenitors Coexpressing *Rag1*-GFP and IL7Rα in E9.5 Embryos

(A) Unfractionated E10.5 (1 FL/recipient), E11.5, and E12.5 (3–4 FLs per recipient) FL cells were competitively transplanted into lethally irradiated wild-type recipients. Left panel, total donor; right panel, myeloid reconstitution (dotted line represents detection level [background staining]; 0.1% donor contribution). Numbers indicate frequencies of mice reconstituted.

(B) Lin$^-$Kit$^+$*Rag1*GFP$^+$IL7Rα^+ cells in E11.5 FL were analyzed for expression of Flt3 (upper panel) and Lin$^-$Kit$^+$Flt3$^+$IL7Rα^+ cells for *Rag1*-GFP expression (lower panel). Mean percentages expression, gray line represents control (representative of 12 embryos investigated).

(C) Coexpression of IL7Rα and *Rag1*-GFP in Lin$^-$Kit$^+$ progenitors in E10.5 (30–38 sp) FL cells. Mean percentage of total cells (5 experiments).

(D) Myeloid (single cells; left panel), megakaryocyte (single cells; middle panel), and erythroid (BFU-E; right panel) potential of Lin$^-$Kit$^+$*Rag1*GFP$^+$IL7Rα^+ E10.5 FL cells. Mean ± SD (>150 cells per assay, 3–5 experiments).

(E) Representative morphology of macrophages (left panel) and granulocytes (right panel) derived from sorted Lin$^-$Kit$^+$*Rag1*GFP$^+$IL7Rα^+ E10.5 FL cells as indicated by arrows.

(F) B cell (NK1.1$^-$CD19$^+$) and (G) T cell (NK1.1$^-$CD25$^+$Thy1.2^{hi} and/or NK1.1$^-$CD4$^+$CD8$^+$) potential (4 cells per well, 3 experiments) of Lin$^-$Kit$^+$*Rag1*GFP$^+$IL7Rα^+ E10.5 FL cells. Mean percentages ± SD.

(H) Lack of expression of IL7Rα and *Rag1*-GFP in the E8.5 (4–7 sp) conceptus. Viable cells were gated negative for mature lineage markers. Middle and right panels show expression analysis on CD45$^-$ and CD45$^+$ cells, respectively (2 experiments).

(I) Coexpression of IL7Rα and *Rag1*-GFP in different tissues at E9.5 (14–26 sp); PAS (left panel), placenta (middle panel), and YS (right panel). Viable cells were gated negative for lineage markers; further gating is indicated with arrows. Mean percentages of total cells (3 experiments).

(J) Expression of CD45, CD41, and VE-Cadherin within the E9.5 YS Lin$^-$Kit$^+$*Rag1*GFP$^+$IL7Rα^+ population. Mean percentages of parent gate (3 experiments).

(K) Single-cell RT-PCR analysis in Lin$^-$Kit$^+$*Rag1*GFP$^+$IL7Rα^+ E9.5 YS progenitors and (L) combined transcriptional lineage priming patterns based on (K). Mean percentages ± SD of total *Kit*$^+$ cells (>91%; ≥50 cells, 2 experiments).

(M) Confocal image of a whole-mount immunolabeled E9.5 (23sp) *Rag1*GFP YS. Arrows indicate GFP$^+$ cells in the vascular plexus coexpressing CD31 and CD45. One of these (boxed area) is enlarged to show fluorescence in the individual channels. Original magnification 250×. Scale bar represents 100 μm.

(N) Left panel shows the number of GFP$^+$ cells per E9.5 YS and embryo proper respectively (mean ± SD, 11–14 embryos). ***$p \leq 0.001$. Right panel shows distribution of GFP$^+$ cells within individual YS analyzed, as cells localized in the vascular plexus or in less branched larger vessels.

(O) Whole embryos at E8.5 and PAS and YS from E9.5 embryos were analyzed for *Rag2* and *Il7r* expression by quantitative PCR. Mean expression ± SD (normalized to *Hprt*; 2–4 biological replicates). *, not detected.

(P) Explant culture of precirculation *Rag1*-GFP YS (≤6 sp), were immunolabeled to detect the presence of *Rag1*GFP$^+$ cells. Representative confocal image of a YS explant (1 sp). The boxed area is enlarged and individual channels are shown for a GFP$^+$ cell coexpressing CD31 and CD45. Original magnification 250×. Scale bar represents 50 μm.

(Q) Precirculation PAS and YS were analyzed after 48 hr explant culture for *Il7r* and *sIgh* expression by quantitative PCR. Mean expression ± SD (normalized to *Hprt*; 3 biological replicates).

See also Figure S3.

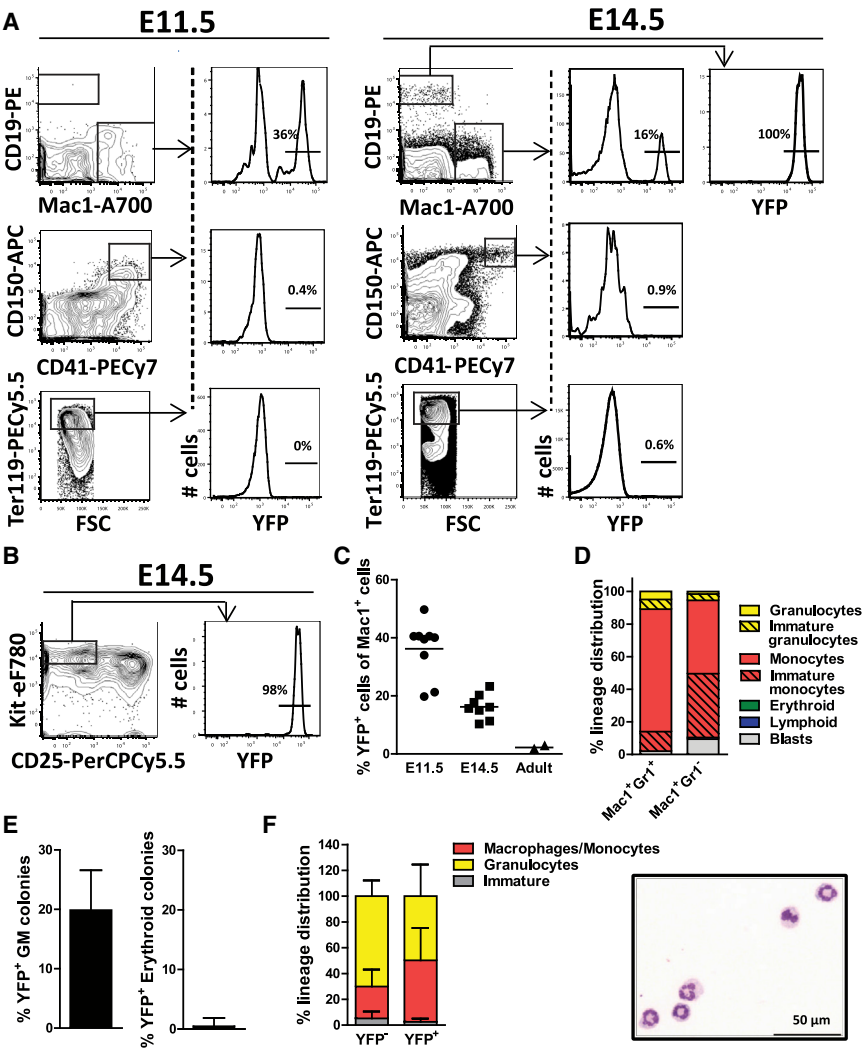

Figure 4. *Rag1* Expressing Immune-Restricted Progenitors Contribute to Embryonic Myelopoiesis

(A) *Rag1-Cre* fate mapping in E11.5 FL and E14.5 FL from *Rag1-Cre*$^{tg/+}$*R26R*$^{eYFP/+}$ embryos. Histograms show percentage of YFP$^+$ cells of total Mac1$^+$ (Ter119$^-$CD150$^-$CD41$^-$) myeloid cells, CD19$^+$ B cells, CD41$^+$CD150$^+$ (Ter119$^-$CD19$^-$Mac1$^-$Gr1$^-$) megakaryocytes, and Ter119$^+$ (CD19$^-$Mac1$^-$Gr1$^-$CD41$^-$CD150$^-$) erythroid cells. Mean percentages of parent gate (8 or 9 embryos).

(B) *Rag1-Cre* fate mapping in E14.5 thymus. Histogram shows percentage of YFP$^+$ cells of Kit$^+$CD25$^+$ (Lin$^-$CD4$^-$CD8$^-$) DN1 thymocytes. Mean percentages of parent gate (4 embryos).

(C) Percentages YFP$^+$ cells of total Mac1$^+$ myeloid cells in E11.5 FL, E14.5 FL, and adult BM. Each dot represents one individual mouse or embryo.

(D) Morphological distribution of cell types within Mac1$^+$Gr1$^+$YFP$^+$ (CD19$^-$B220$^-$Ter119$^-$CD150$^-$CD41$^-$) and Mac1$^+$Gr1$^-$YFP$^+$ (CD19$^-$B220$^-$Ter119$^-$CD150$^-$CD41$^-$) cells sorted from *Rag1-Cre*$^{tg/+}$*R26R*$^{eYFP/+}$ E14.5 FLs. Mean percentages (2 experiments).

(E) Mean percentages ± SD of YFP$^+$ GM (left) and erythroid (right) colonies generated from unfractionated E14.5 *Rag1-Cre*$^{tg/+}$*R26R*$^{eYFP/+}$ FL cells (GM; 12 individual embryos, >1000 colonies, Erythroid; 9 individual embryos, 218 colonies).

(F) Morphological distribution of cell types within YFP$^-$ and YFP$^+$ myeloid colonies generated from E14.5 *Rag1-Cre*$^{tg/+}$*R26R*$^{eYFP/+}$ FL cells in semi-solid culture. Mean percentage ± SD (5 embryos). Right panel shows representative granulocytes from YFP$^+$ colony.

See also Figure S4.

DISCUSSION

Although other recent studies have carefully documented the emergence of progenitors with substantial lymphoid potential already in the E9.5 YS, as evaluated in cultures and upon transplantation (Yoshimoto et al., 2012), it has remained unclear whether or not this lymphoid potential comes from a multipotent progenitor in the YS or an already partially or fully lymphoid-restricted progenitor. *Ncx1* knockout embryos fail to develop a beating heart and therefore lack a circulation. Investigation of *Ncx1* null embryos provided compelling evidence for the emergence in the YS of progenitors with considerable lymphoid potential as established through their ability in long-term cultures and upon transplantation to produce fetal, as well as adult type, T cells (Yoshimoto et al., 2012). However, the progenitors responsible for this activity were not prospectively identified, and it was not established whether the cells producing only T cells in the long-term assays might also possess other lineage potentials. In fact, in another study it was shown that the same E9.5 YS cells also have B cell potential when assessed in other assays (Yoshimoto et al., 2011). The present studies suggest that the T and B lymphoid potential observed in the E9.5 YS by Yoshimoto et al. might derive at least in part from multipotent but lympho-myeloid-restricted progenitors.

Through prospective purification, molecular characterization, and fate mapping, the findings herein establish that extensive lymphoid transcriptional priming and lymphomyeloid-lineage restriction initiates in the YS at E9.5, earlier than previously recognized, before the emergence of definitive HSCs and establishment of FL hematopoiesis. This restriction occurs through the establishment of distinct immune-restricted progenitors with combined lymphoid and myeloid lineage potentials (Figure 7), defined by upregulation of specific regulators of lymphopoiesis: *Rag1*, Flt3, and IL7Rα, as well as a number of other lymphoid-specific transcripts. Importantly, single-cell lineage-potential assays, as well as in vivo fate mapping of their progeny during normal embryonic development, confirmed not only the virtual absence of MkE potentials but also the physiological and robust contribution to the myeloid (GM), as well as lymphoid, lineages in the developing embryo.

The lymphomyeloid-primed progenitors already detected in E9.5 YS and E10.5 FL represent the earliest identified embryonic progenitors in which specific and key lymphoid gene expression is initiated, coexpressed with myeloid genes, and paralleled by a distinct downregulation of MkE genes, similar to the LMPPs

identified later in development (Adolfsson et al., 2005; Månsson et al., 2007). The lymphoid genes expressed in these embryonic progenitors were early common lymphoid genes, whereas early B and T cell progenitor-specific genes were found to be negative, in agreement with previous studies supporting that B and T cell lineage commitment occurs later in FL hematopoiesis (Douagi et al., 2002), or at least not within the herein identified lymphomyeloid-restricted progenitors. Moreover, every $Lin^{-}Kit^{+}Flt3^{+}IL7R\alpha^{+}$ progenitor cell expressing these lymphoid genes coexpressed at the single-cell level myeloid lineage genes even in the E11.5 FL, whereas none of them expressed signature genes of the earliest B (*Pax5*) and T (*Ptcra*) cell-restricted progenitors. In light of these findings, we suggest that earlier studies implicating the emergence of fully B or T lymphoid-restricted progenitors already in the E10–10.5 AGM region and fetal circulation, based on evaluation of clonal lineage output of heterogenous progenitor populations (Ikawa et al., 2004; Ohmura et al., 1999), might have missed the myeloid output of lymphomyeloid-restricted progenitors as a result of the short lifespan of myeloid cells in culture. Regardless, establishment of whether also fully lymphoid-restricted progenitors might emerge prior to definitive HSCs would require their prospective purification and molecular evidence of fully lymphoid-restricted progenitor cells.

The most significantly upregulated genes in embryonic lymphomyeloid-restricted progenitors were almost exclusively related to development or function of the immune system, including genes demonstrated to be of critical importance for establishment of thymopoiesis (Rothenberg, 2007), implicating early embryonic lymphomyeloid progenitors as candidate TSPs. Findings of Yoshimoto et al. (2012) showing that there are cells with thymus reconstitution potential already in the E9.5 YS and PAS region, combined with our identification in E9.5 YS of distinct lymphomyeloid-primed progenitors with upregulated expression of genes for chemokine receptors, critically involved in migration of TSPs to the embryonic thymus, raises the possibility that TSPs responsible for initiation of thymopoiesis in the embryo might be generated in the YS.

Our analysis of different hematopoietic regions in the embryo by FACS, whole-mount imaging, and PCR analysis suggest that the identified lymphomyeloid-restricted progenitors emerge first in the YS at E9.5, a finding further supported by precirculation explant short-term cultures of the YS and PAS regions. The identity of the hematopoietic stem-progenitor cells giving rise to this first wave of lymphomyeloid-restricted progenitors remains to be established. Although their early emergence rules out an origin from definitive HSCs, they might derive from hemogenic endothelium in E9.5 YS as suggested in recent studies (Yoshimoto et al., 2012) and as further supported by our finding of *Rag1*GFP^{+} cells in the primitive vascular plexus in the E9.5 YS. Alternatively, they might derive from multipotent progenitors in the YS, also possessing MkE potential, or potentially from recently identified candidate pre-HSCs (Figure 7B).

Previous studies have proposed the existence of mouse lymphomyeloid-restricted progenitors in FL hematopoiesis (Cumano et al., 1992; Katsura and Kawamoto, 2001; Lacaud et al., 1998), and the LMPP was later prospectively identified in adult hematopoiesis as well as in E14.5 FL (Adolfsson et al., 2005; Arinobu et al., 2007; Månsson et al., 2007). Although collectively these studies provided compelling experimental support for a revised hematopoietic hierarchy with separate CMP and lymphomyeloid immune-restricted pathways (reviewed in (Luc et al., 2008b), this has not precluded the conceptually classical CMP-CLP roadmap from still prevailing in the literature (Orkin and Zon, 2008a, b; Seita and Weissman, 2010). This controversy reflects in part that all studies supporting either model have relied exclusively on the ability of nonphysiological in vitro and in vivo reconstitution assays to uncover lineage potentials of the prospectively purified progenitor cells. Thus, although these studies have been instrumental for our current understanding of lineage commitment, the assays applied do have intrinsic caveats (Richie Ehrlich et al., 2011). Perhaps even more relevant, uncovering of multiple lineage potentials of a progenitor cell in vitro or upon in vivo transplantation into conditioned recipients does not address whether and to what degree the progenitor in question contributes (or not) under normal in vivo physiological conditions toward the different cell lineage potentials.

Although genetic fate-mapping experiments in vivo could address these fundamentally important questions, it remains a considerable challenge to develop strategies that would faithfully allow lineage tracing of distinct progenitor cells. Results from recent *Flt3* lineage-tracing studies questioned the physiological relevance of an early lymphomyeloid lineage-restriction step in hematopoiesis (Boyer et al., 2011, 2012), although the conclusions were limited by *Flt3* expression initiating already in fully multipotent progenitors (Boyer et al., 2012; Buza-Vidas et al., 2011). Another recent *Il7r* fate-mapping study also questioned the myeloid contribution and the physiological significance of a lymphomyeloid-restricted pathway (Schlenner et al., 2010; Schlenner and Rodewald, 2010), as did *Rag1* fate mapping in adult hematopoiesis (Welner et al., 2009). However, only a small fraction of adult lymphomyeloid-restricted LMPPs express *Il7r* or *Rag1* (Adolfsson et al., 2005; Luc et al., 2008a), and $Rag1^{+}$ LMPPs have considerably reduced myeloid potential as compared to $Rag1^{-}$ LMPPs (Luc et al., 2008a). In contrast, we here demonstrate that early embryonic lymphomyeloid-restricted progenitors express much higher levels of *Il7r* and *Rag1*, and when applying *Rag1-Cre* fate mapping, we could for the first time demonstrate that lymphomyeloid-restricted progenitors contribute extensively to myelopoiesis, as well as lymphopoiesis during normal fetal development. Of equal importance, we found no significant contribution of *Rag1*-expressing progenitors to the MkE lineages in vivo, confirming their immune-restricted role. Thus, our combined lineage potential and fate-mapping studies establish the existence of lymphomyeloid-restricted progenitors in early embryonic hematopoiesis prior to emergence of definitive HSCs, and their physiological contribution to both the myeloid innate and lymphoid adaptive immune system. Notably, the existence of lymphomyeloid-restricted progenitors has also recently been implicated in early postnatal and adult human hematopoiesis (Doulatov et al., 2010; Goardon et al., 2011; Kohn et al., 2012).

The identification of an embryonic immune-restricted progenitor is of relevance for childhood acute lymphoblastic leukemia (cALL), the most common form of pediatric cancer. Preleukemic translocations in cALL frequently occur in utero in unidentified

Please cite this article in press as: Böiers et al., Lymphomyeloid Contribution of an Immune-Restricted Progenitor Emerging Prior to Definitive Hematopoietic Stem Cells, Cell Stem Cell (2013), http://dx.doi.org/10.1016/j.stem.2013.08.012

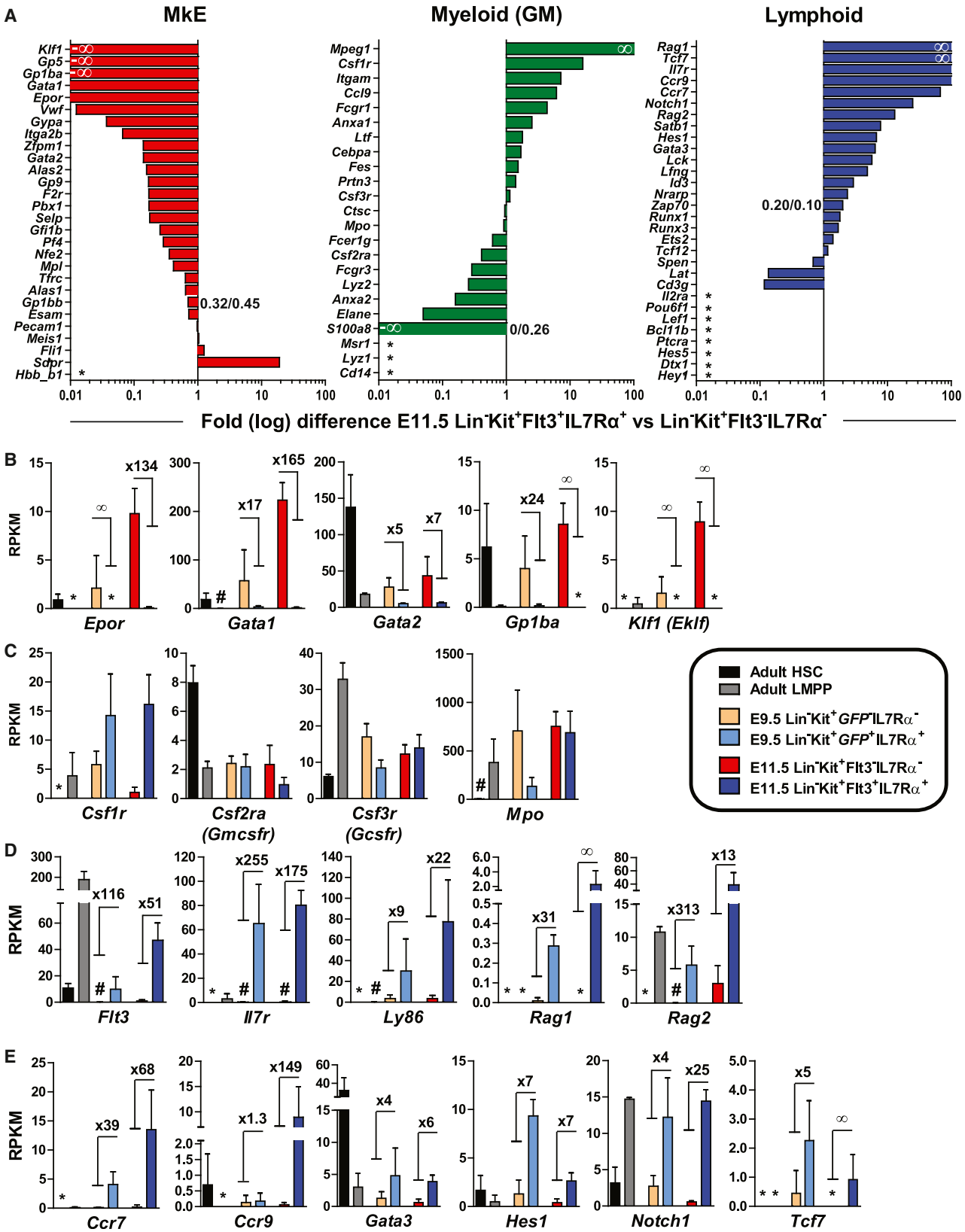

(legend on next page)

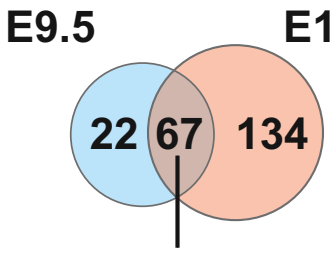

Statistically over-represented Gene Ontology Categories

GO annotation	FDR	Coverage
B cell activation	2.42E-02	6 / 147
immunoglobulin production	2.42E-02	5 / 69
T cell differentiation	2.42E-02	6 / 154
external side of plasma membrane	2.42E-02	7 / 229
production of molecular mediator of immune response	3.34E-02	5 / 97
T cell activation	3.93E-02	7 / 274
B cell proliferation	6.68E-02	4 / 60
lymphocyte differentiation	6.68E-02	6 / 203
regulation of lymphocyte differentiation	2.68E-01	4 / 88
leukocyte differentiation	3.80E-01	6 / 296

Commonly upregulated genes in E9.5 and E11.5 immune-restricted progenitors

2010001M09Rik	*Clec12a*	*Gem*	*Ift57*	*Mycn*	*Ptprc*	*Stc1*
Abcg3	*Ctnnd2*	*Gimap6*	*Il1r2*	*Napsa*	*Pygm*	*Tifa*
Alcam	*Cybb*	*Gimap7*	*Il7r*	*Notch1*	*Rag2*	*Tnip3*
Bfsp2	*Dpysl2*	*Gngt2*	*Klrd1*	*P2ry12*	*Rgs1*	*Tnni2*
Calcrl	*Dusp6*	*Gpr171*	*Lax1*	*P2ry14*	*Runx2*	*Tsc22d1*
Ccnd2	*Emcn*	*Gpr65*	*Lsp1*	*Plk2*	*Serpinb1a*	*Tshz3*
Cd27	*Entpd1*	*Gsn*	*Ly86*	*Ppp1r16b*	*Sesn1*	*Zcchc18*
Cd33	*Ets1*	*Hmgn3*	*Marcks*	*Prss2*	*Snn*	
Cd7	*Fgd2*	*Ifi203*	*Mn1*	*Psmb8*	*Sp100*	
Cdh17	*Flt3*	*Ifitm3*	*Mndal*	*Psmb9*	*St8sia4*	

Figure 6. Upregulation of Immune-Related Genes in E9.5 Yolk Sac and E11.5 Fetal Liver Immune-Restricted Progenitors

Venn diagram showing overlap of upregulated genes in E9.5 YS Lin$^-$Kit$^+$ *Rag1*GFP$^+$IL7Rα^+ (compared to Lin$^-$Kit$^+$*Rag1*GFP$^-$IL7Rα^-) cells and E11.5 FL Lin$^-$Kit$^+$Flt3$^+$IL7Rα^+ (compared to Lin$^-$Kit$^+$Flt3$^-$IL7Rα^-) cells. Of these 67 overlapping genes, 64 were also upregulated in E10.5 FL Lin$^-$Kit$^+$ *Rag1*GFP$^+$IL7Rα^+ cells (data not shown). Also shown are Gene Ontology Categories in which common upregulated genes were significantly enriched. Note that almost all of these categories are related to the immune system. See also Figures S5 and S6 and Tables S1–S3.

progenitors (Greaves and Wiemels, 2003), also resulting in poor-prognosis biphenotypic leukemias with characteristics of the lymphoid and the GM, but not MkE lineages (Béné, 2009). Our identification of immune-restricted progenitors emerging in the embryo prior to definitive HSCs and establishment of FL hematopoiesis will also facilitate a better understanding of the molecular determinants and cellular pathways required for the development of a fully competent innate and adaptive immune system and of how this process is dysregulated in the conglomerate of congenital immune deficiencies (Cunningham-Rundles and Ponda, 2005).

EXPERIMENTAL PROCEDURES

Animals and Cell Preparations

Embryos were obtained by timed mating, with the morning of vaginal plug detection set as E0.5. Animal experiments were performed according to regulations by the local animal ethics committee at Lund University and the UK Home Office at University of Oxford. For details, see Supplemental Experimental Procedures.

Fluorescence Activated Cell Sorting

Dissected tissues and adult BM (>8 weeks old) were treated with purified anti-CD16/32 (Fc-block) and stained with antibodies specified in Supplemental Experimental Procedures. Adult HSCs and progenitors were defined with the following markers: adult HSCs; LSKCD150$^+$CD48$^-$, LMPPs; LSKFlt3^{hi}, CLPs; Lin$^-$CD11c$^-$Ly6C$^-$CD19$^-$B220$^-$Ly6D$^-$Kit^{lo}Sca^{lo}Flt3$^+$IL7Rα^+; proB cells; Kit$^+$CD19$^+$B220$^+$CD43$^+$.

In Vitro Cultures

Evaluation of MkE and GM lineage potentials was performed as previously described with minor modifications (Supplemental Experimental Procedures) (Adolfsson et al., 2005; Luc et al., 2008a; Månsson et al., 2007). Erythroid lineage potential was additionally evaluated on Op9 coculture with cytokines as specified in Supplemental Experimental Procedures. Clones were considered positive for erythroid development if cells had a Ter119$^+$CD71$^+$ (Mac1$^-$Gr1$^-$CD150$^-$CD41$^-$) FACS profile and/or by positive morphology on May-Grünwald/Giemsa stained cytospins. For evaluation of lymphoid potential or combined potential, cells were plated onto Op9 or Op9DL1 stroma cells with cytokines as previously described (Månsson et al., 2007) (see Supplemental Experimental Procedures).

Rag1-Cre Fate Mapping

Rag1-Cre$^{tg/+}$*R26R*$^{eYFP/+}$ and littermate *Rag1-Cre*$^{+/+}$*R26R*$^{eYFP/+}$ control adult BM and FLs (E11.5 and E14.5) were stained as specified in Supplemental Experimental Procedures. Adult *Flt3-Cre*$^{tg/+}$*R26R*$^{eYFP/+}$ BM was used as a positive control to demonstrate that the R26 promoter sustains YFP expression in all mature (B, T, Mk, and E) lineages as previously shown (Buza-Vidas et al., 2011) (for further details, see Supplemental Experimental Procedures).

Explant Cultures and Imaging

The YS and PAS regions were dissected from staged embryos ($\leq$6 sp) prior to establishment of circulation as previously described (Cumano et al., 1996), cultured individually, and then whole-mount immunolabeled, or explants were taken for quantitative PCR (see Supplemental Experimental Procedures).

In Vivo Reconstitution Experiments

FL cells from E10.5 (32–44 sp), E11.5, and E12.5 CD45.2 embryos were transplanted together with 250,000–300,000 competitor CD45.1 BM cells into lethally irradiated (2 × 450cGy) C57/Bl6 WT CD45.1 mice, either intravenously or intrafemorally as specified (in some cases CD45.1 embryos were used and transplanted into CD45.2 WT recipients). Peripheral blood (PB) analyses were conducted at 15–17 weeks (see Supplemental Experimental Procedures). Mice were considered reconstituted if $\geq$0.1% donor contribution to total CD45$^+$ cells was achieved.

Figure 5. Upregulation of Lymphoid and Downregulation of MkE Transcriptional Programs in Early Embryonic Immune-Restricted Progenitors

(A) E11.5 Lin$^-$Kit$^+$Flt3$^+$IL7Rα^+ and Lin$^-$Kit$^+$Flt3$^-$IL7Rα^- E11.5 FL cells were subjected to global RNA sequencing and analyzed for differences in expression levels of previously published lineage-associated (MkE, Myeloid [GM], and Lymphoid) programs (Luc et al., 2012). Mean fold differences in RPKM (= reads per kilobase of exon model per million mapped reads) values are shown on a $\log_{10}$ scale. *, RPKM $\leq$0.05 for both cell populations. For genes with expression $\leq$0.5 RPKM for both cell populations, specific values are indicated next to bars. ∞, infinity.

(B–E) Expression as determined by RNA sequencing of (B) MkE, (C) GM, (D) lymphoid, and (E) thymus-seeding progenitor related genes, in E9.5 YS and E11.5 FL progenitors. Adult HSCs and adult LMPPs are shown as controls. Graph legend for (B)–(E) is shown in the box to the right. Numbers indicate fold difference. Mean RPKM ± SD (2–3 experiments).

*, not detected; #, expressed but at too low level to be visualized on the applied scale; and ∞, infinity as not detected in one of the two cell populations in either experiment.

See also Figures S5 and S6.

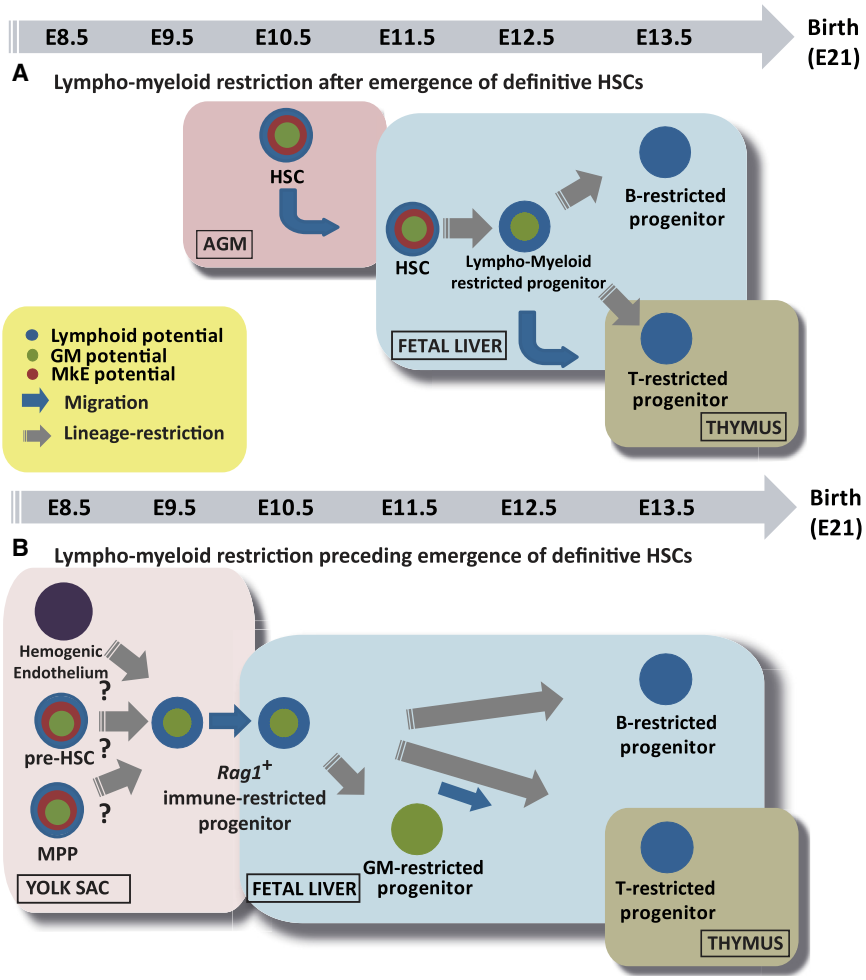

Figure 7. Lymphoid-Myeloid Lineage Restriction in the Mouse Embryo Occurs Independently of and Precedes Emergence of Definitive HSCs

(A) Lymphomyeloid lineage restriction after emergence of definitive HSCs. Model for initiation of lymphomyeloid lineage restriction based on published data suggesting that the first lymphoid restriction steps occurs after emergence of definitive HSCs in the aorta-gonad-mesonephros (AGM) region and their subsequent seeding of the fetal liver. According to this model, the first lympho-myeloid progenitors (for which the exact lineage potentials at the single-cell level remains unclear) emerge at about E12 followed by generation of B and T lymphoid restricted progenitors at E13.5 or later.

(B) Initiation of lymphomyeloid lineage restriction preceding emergence of definitive HSCs. Initiation of lymphomyeloid lineage restriction based on the identification of a *Rag1*GFP^{+}IL7Rα^{+} immune-restricted progenitor at E9.5 in yolk sac and E10.5 in fetal liver, prior to emergence of definitive HSCs in the AGM region. This early immune-restricted progenitor contributes to myelopoiesis (GM) already at E11.5 and later to B and T cell restricted progenitors but little or not to megakaryo-erythropoiesis. The immune-restricted progenitor emerges in the yolk sac prior to definitive HSCs, which is compatible with originating from proposed hemogenic endothelium, pre-HSCs, or earlier multipotent progenitors, as indicated.

Single-Cell and Quantitative PCR

Multiplex single-cell RT-PCR and multiplex quantitative real-time PCR analysis (BioMark 48.48 or 96.96 Dynamic Array platform [Fluidigm] with TaqMan Gene Expression Assays [Applied Biosystems]) were performed as described in Supplemental Experimental Procedures (Adolfsson et al., 2005; Månsson et al., 2007).

RNA Sequencing

Samples for RNA sequencing (73–100 cells) were prepared with the SMARTer Ultra Low RNA kit for Illumina Sequencing (Clontech) and sequenced and analyzed as previously described (Ramsköld et al., 2012) (see Supplemental Experimental Procedures).

Statistics

Statistical significance was determined by one or two-tailed (depending on hypothesis) unpaired Mann Whitney (nonparametric) test. The significance level was set at $p \leq 0.05$. Unless otherwise stated, data are shown as mean ± SD.

ACCESSION NUMBERS

The RNA sequencing data have been deposited in NCBI GEO under accession number GSE50896.

SUPPLEMENTAL INFORMATION

Supplemental Information includes six figures, three tables, and Supplemental Experimental Procedures and can be found with this article online at http://dx.doi.org/10.1016/j.stem.2013.08.012.

AUTHOR CONTRIBUTIONS

S.E.W.J. and C.B. conceptualized and designed the overall research, analyzed the data, and wrote the manuscript. C.B., M.L., S.L., A.H., J.C., and J.C.A.G. performed and analyzed experiments. M.L. did the micromanipulation of single cells. E.A., G.S., and M.B. performed the embryonic dissections; E.A. performed the whole mount imaging and M.B. contributed with expert advice and input on design and analysis of embryonic studies. I.G. performed and designed the explant culture experiments. P.S.W., I.C.M., Q.D., and R.S. performed and analyzed the RNA sequencing data. D.A. and A.J.M. performed and analyzed the quantitative PCR data, and A.J.M. analyzed morphology. T.B.-J. and L.M. contributed in vitro culture experiments. T.C.L. analyzed transplantation experiments, and S.K., A.P., and C.T.J. contributed and performed the initiating experiments of the study. E.G.P. and F.G. performed and analyzed the tissue macrophage experiments. E.S. contributed with advice on execution of experiments. All authors read and approved the final manuscript.

ACKNOWLEDGMENTS

The authors thank Lilian Wittmann, Ingbritt Åstrand-Grundström, and Hanane Boukarabila for skillful technical assistance, the Biomedical Services at Oxford University for expert animal support, and Sally-Ann Clark, Paul Sopp, and the WIMM FACS facility for FACS support. Åsa Björklund, Daniel Ramsköld, and Ersen Kavak are thanked for skillful technical assistance with the RNA sequencing. This work was supported by a programme grant (H4RPLK0) from the Medical Research Council UK (S.E.W.J.), Knut och Alice

Wallenberg Foundation (WIRM; S.E.W.J.), StratRegen, KI (S.E.W.J.), EU-FP7 EuroSyStem Integrated projects (S.E.W.J.), ALF (Government Public Health Grant; C.B.), the Hemato-Linné grant (Swedish Research Council Linnaeus; S.E.W.J.), the MRC Molecular Haematology Unit core award (M.F.T.R.d.-B., E.A., S.E.W.J.), a Leukaemia and Lymphoma Research project grant (M.B., G.S.), Swedish Cancer foundation (A.H.), Swedish Society of Medicine (A.H.), Crafoord Foundation (A.H.), Georg Danielsson's foundation (A.H.), and the Leukaemia and Lymphoma Research Senior Bennett Fellowship (A.J.M.).

Received: February 16, 2013
Revised: July 21, 2013
Accepted: August 28, 2013
Published: September 19, 2013

REFERENCES

Adolfsson, J., Månsson, R., Buza-Vidas, N., Hultquist, A., Liuba, K., Jensen, C.T., Bryder, D., Yang, L., Borge, O.J., Thoren, L.A., et al. (2005). Identification of Flt3+ lympho-myeloid stem cells lacking erythro-megakaryocytic potential a revised road map for adult blood lineage commitment. Cell *121*, 295–306.

Akashi, K., Traver, D., Miyamoto, T., and Weissman, I.L. (2000). A clonogenic common myeloid progenitor that gives rise to all myeloid lineages. Nature *404*, 193–197.

Arinobu, Y., Mizuno, S., Chong, Y., Shigematsu, H., Iino, T., Iwasaki, H., Graf, T., Mayfield, R., Chan, S., Kastner, P., and Akashi, K. (2007). Reciprocal activation of GATA-1 and PU.1 marks initial specification of hematopoietic stem cells into myeloerythroid and myelolymphoid lineages. Cell Stem Cell *1*, 416–427.

Béné, M.C. (2009). Biphenotypic, bilineal, ambiguous or mixed lineage: strange leukemias! Haematologica *94*, 891–893.

Boyer, S.W., Schroeder, A.V., Smith-Berdan, S., and Forsberg, E.C. (2011). All hematopoietic cells develop from hematopoietic stem cells through Flk2/Flt3-positive progenitor cells. Cell Stem Cell *9*, 64–73.

Boyer, S.W., Beaudin, A.E., and Forsberg, E.C. (2012). Mapping differentiation pathways from hematopoietic stem cells using Flk2/Flt3 lineage tracing. Cell Cycle *11*, 3180–3188.

Buza-Vidas, N., Woll, P., Hultquist, A., Duarte, S., Lutteropp, M., Bouriez-Jones, T., Ferry, H., Luc, S., and Jacobsen, S.E. (2011). FLT3 expression initiates in fully multipotent mouse hematopoietic progenitor cells. Blood *118*, 1544–1548.

Cumano, A., Paige, C.J., Iscove, N.N., and Brady, G. (1992). Bipotential precursors of B cells and macrophages in murine fetal liver. Nature *356*, 612–615.

Cumano, A., Dieterlen-Lievre, F., and Godin, I. (1996). Lymphoid potential, probed before circulation in mouse, is restricted to caudal intraembryonic splanchnopleura. Cell *86*, 907–916.

Cunningham-Rundles, C., and Ponda, P.P. (2005). Molecular defects in T- and B-cell primary immunodeficiency diseases. Nat. Rev. Immunol. *5*, 880–892.

Douagi, I., Vieira, P., and Cumano, A. (2002). Lymphocyte commitment during embryonic development, in the mouse. Semin. Immunol. *14*, 361–369.

Doulatov, S., Notta, F., Eppert, K., Nguyen, L.T., Ohashi, P.S., and Dick, J.E. (2010). Revised map of the human progenitor hierarchy shows the origin of macrophages and dendritic cells in early lymphoid development. Nat. Immunol. *11*, 585–593.

Forsberg, E.C., Serwold, T., Kogan, S., Weissman, I.L., and Passegué, E. (2006). New evidence supporting megakaryocyte-erythrocyte potential of flk2/flt3+ multipotent hematopoietic progenitors. Cell *126*, 415–426.

Goardon, N., Marchi, E., Atzberger, A., Quek, L., Schuh, A., Soneji, S., Woll, P., Mead, A., Alford, K.A., Rout, R., et al. (2011). Coexistence of LMPP-like and GMP-like leukemia stem cells in acute myeloid leukemia. Cancer Cell *19*, 138–152.

Greaves, M.F., and Wiemels, J. (2003). Origins of chromosome translocations in childhood leukaemia. Nat. Rev. Cancer *3*, 639–649.

Hu, M., Krause, D., Greaves, M., Sharkis, S., Dexter, M., Heyworth, C., and Enver, T. (1997). Multilineage gene expression precedes commitment in the hemopoietic system. Genes Dev. *11*, 774–785.

Ikawa, T., Masuda, K., Lu, M., Minato, N., Katsura, Y., and Kawamoto, H. (2004). Identification of the earliest prethymic T-cell progenitors in murine fetal blood. Blood *103*, 530–537.

Katsura, Y., and Kawamoto, H. (2001). Stepwise lineage restriction of progenitors in lympho-myelopoiesis. Int. Rev. Immunol. *20*, 1–20.

Kawamoto, H., Ikawa, T., Ohmura, K., Fujimoto, S., and Katsura, Y. (2000). T cell progenitors emerge earlier than B cell progenitors in the murine fetal liver. Immunity *12*, 441–450.

Kieusseian, A., Brunet de la Grange, P., Burlen-Defranoux, O., Godin, I., and Cumano, A. (2012). Immature hematopoietic stem cells undergo maturation in the fetal liver. Development *139*, 3521–3530.

Kohn, L.A., Hao, Q.L., Sasidharan, R., Parekh, C., Ge, S., Zhu, Y., Mikkola, H.K., and Crooks, G.M. (2012). Lymphoid priming in human bone marrow begins before expression of CD10 with upregulation of L-selectin. Nat. Immunol. *13*, 963–971.

Kondo, M., Weissman, I.L., and Akashi, K. (1997). Identification of clonogenic common lymphoid progenitors in mouse bone marrow. Cell *91*, 661–672.

Kumaravelu, P., Hook, L., Morrison, A.M., Ure, J., Zhao, S., Zuyev, S., Ansell, J., and Medvinsky, A. (2002). Quantitative developmental anatomy of definitive haematopoietic stem cells/long-term repopulating units (HSC/RUs): role of the aorta-gonad-mesonephros (AGM) region and the yolk sac in colonisation of the mouse embryonic liver. Development *129*, 4891–4899.

Lacaud, G., Carlsson, L., and Keller, G. (1998). Identification of a fetal hematopoietic precursor with B cell, T cell, and macrophage potential. Immunity *9*, 827–838.

Liu, C., Saito, F., Liu, Z., Lei, Y., Uehara, S., Love, P., Lipp, M., Kondo, S., Manley, N., and Takahama, Y. (2006). Coordination between CCR7- and CCR9-mediated chemokine signals in prevascular fetal thymus colonization. Blood *108*, 2531–2539.

Luc, S., Anderson, K., Kharazi, S., Buza-Vidas, N., Böiers, C., Jensen, C.T., Ma, Z., Wittmann, L., and Jacobsen, S.E. (2008a). Down-regulation of Mpl marks the transition to lymphoid-primed multipotent progenitors with gradual loss of granulocyte-monocyte potential. Blood *111*, 3424–3434.

Luc, S., Buza-Vidas, N., and Jacobsen, S.E. (2008b). Delineating the cellular pathways of hematopoietic lineage commitment. Semin. Immunol. *20*, 213–220.

Luc, S., Luis, T.C., Boukarabila, H., Macaulay, I.C., Buza-Vidas, N., Bouriez-Jones, T., Lutteropp, M., Woll, P.S., Loughran, S.J., Mead, A.J., et al. (2012). The earliest thymic T cell progenitors sustain B cell and myeloid lineage potential. Nat. Immunol. *13*, 412–419.

Månsson, R., Hultquist, A., Luc, S., Yang, L., Anderson, K., Kharazi, S., Al-Hashmi, S., Liuba, K., Thorén, L., Adolfsson, J., et al. (2007). Molecular evidence for hierarchical transcriptional lineage priming in fetal and adult stem cells and multipotent progenitors. Immunity *26*, 407–419.

Masuda, K., Kubagawa, H., Ikawa, T., Chen, C.C., Kakugawa, K., Hattori, M., Kageyama, R., Cooper, M.D., Minato, N., Katsura, Y., and Kawamoto, H. (2005). Prethymic T-cell development defined by the expression of paired immunoglobulin-like receptors. EMBO J. *24*, 4052–4060.

Medvinsky, A., and Dzierzak, E. (1996). Definitive hematopoiesis is autonomously initiated by the AGM region. Cell *86*, 897–906.

Medvinsky, A., Rybtsov, S., and Taoudi, S. (2011). Embryonic origin of the adult hematopoietic system: advances and questions. Development *138*, 1017–1031.

Ohmura, K., Kawamoto, H., Fujimoto, S., Ozaki, S., Nakao, K., and Katsura, Y. (1999). Emergence of T, B, and myeloid lineage-committed as well as multipotent hemopoietic progenitors in the aorta-gonad-mesonephros region of day 10 fetuses of the mouse. J. Immunol. *163*, 4788–4795.

Orkin, S.H., and Zon, L.I. (2008a). Hematopoiesis: an evolving paradigm for stem cell biology. Cell *132*, 631–644.

Orkin, S.H., and Zon, L.I. (2008b). SnapShot: hematopoiesis. Cell *132*, 712.

Osawa, M., Hanada, K.-I., Hamada, H., and Nakauchi, H. (1996). Long-term lymphohematopoietic reconstitution by a single CD34-low/negative hematopoietic stem cell. Science *273*, 242–245.

Owen, J.J., and Ritter, M.A. (1969). Tissue interaction in the development of thymus lymphocytes. J. Exp. Med. *129*, 431–442.

Ramsköld, D., Luo, S., Wang, Y.C., Li, R., Deng, Q., Faridani, O.R., Daniels, G.A., Khrebtukova, I., Loring, J.F., Laurent, L.C., et al. (2012). Full-length mRNA-Seq from single-cell levels of RNA and individual circulating tumor cells. Nat. Biotechnol. *30*, 777–782.

Richie Ehrlich, L.I., Serwold, T., and Weissman, I.L. (2011). In vitro assays misrepresent in vivo lineage potentials of murine lymphoid progenitors. Blood *117*, 2618–2624.

Rothenberg, E.V. (2007). Negotiation of the T lineage fate decision by transcription-factor interplay and microenvironmental signals. Immunity *26*, 690–702.

Rybtsov, S., Sobiesiak, M., Taoudi, S., Souilhol, C., Senserrich, J., Liakhovitskaia, A., Ivanovs, A., Frampton, J., Zhao, S., and Medvinsky, A. (2011). Hierarchical organization and early hematopoietic specification of the developing HSC lineage in the AGM region. J. Exp. Med. *208*, 1305–1315.

Schlenner, S.M., and Rodewald, H.R. (2010). Early T cell development and the pitfalls of potential. Trends Immunol. *31*, 303–310.

Schlenner, S.M., Madan, V., Busch, K., Tietz, A., Läufle, C., Costa, C., Blum, C., Fehling, H.J., and Rodewald, H.R. (2010). Fate mapping reveals separate origins of T cells and myeloid lineages in the thymus. Immunity *32*, 426–436.

Schulz, C., Gomez Perdiguero, E., Chorro, L., Szabo-Rogers, H., Cagnard, N., Kierdorf, K., Prinz, M., Wu, B., Jacobsen, S.E., Pollard, J.W., et al. (2012). A lineage of myeloid cells independent of Myb and hematopoietic stem cells. Science *336*, 86–90.

Seita, J., and Weissman, I.L. (2010). Hematopoietic stem cell: self-renewal versus differentiation. Wiley Interdiscip Rev Syst Biol Med *2*, 640–653.

Sitnicka, E., Brakebusch, C., Martensson, I.L., Svensson, M., Agace, W.W., Sigvardsson, M., Buza-Vidas, N., Bryder, D., Cilio, C.M., Ahlenius, H., et al. (2003). Complementary signaling through flt3 and interleukin-7 receptor alpha is indispensable for fetal and adult B cell genesis. J. Exp. Med. *198*, 1495–1506.

Solar, G.P., Kerr, W.G., Zeigler, F.C., Hess, D., Donahue, C., de Sauvage, F.J., and Eaton, D.L. (1998). Role of c-mpl in early hematopoiesis. Blood *92*, 4–10.

Welner, R.S., Esplin, B.L., Garrett, K.P., Pelayo, R., Luche, H., Fehling, H.J., and Kincade, P.W. (2009). Asynchronous RAG-1 expression during B lymphopoiesis. J. Immunol. *183*, 7768–7777.

Ye, M., and Graf, T. (2007). Early decisions in lymphoid development. Curr. Opin. Immunol. *19*, 123–128.

Yokota, T., Huang, J., Tavian, M., Nagai, Y., Hirose, J., Zúñiga-Pflücker, J.C., Péault, B., and Kincade, P.W. (2006). Tracing the first waves of lymphopoiesis in mice. Development *133*, 2041–2051.

Yoshimoto, M., Montecino-Rodriguez, E., Ferkowicz, M.J., Porayette, P., Shelley, W.C., Conway, S.J., Dorshkind, K., and Yoder, M.C. (2011). Embryonic day 9 yolk sac and intra-embryonic hemogenic endothelium independently generate a B-1 and marginal zone progenitor lacking B-2 potential. Proc. Natl. Acad. Sci. USA *108*, 1468–1473.

Yoshimoto, M., Porayette, P., Glosson, N.L., Conway, S.J., Carlesso, N., Cardoso, A.A., Kaplan, M.H., and Yoder, M.C. (2012). Autonomous murine T-cell progenitor production in the extra-embryonic yolk sac before HSC emergence. Blood *119*, 5706–5714.

Yuan, J., Nguyen, C.K., Liu, X., Kanellopoulou, C., and Muljo, S.A. (2012). Lin28b reprograms adult bone marrow hematopoietic progenitors to mediate fetal-like lymphopoiesis. Science *335*, 1195–1200.

Cell Stem Cell, Volume *13*

Supplemental Information

Lymphomyeloid Contribution of an Immune-Restricted Progenitor Emerging Prior to Definitive Hematopoietic Stem Cells

Supplemental Inventory

SUPPLEMENTAL FIGURES

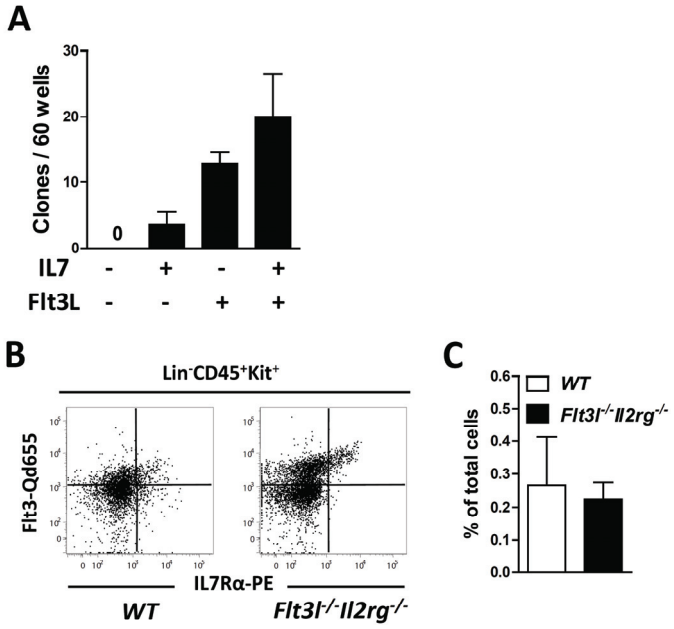

Figure S1 (related to main Figure 1)
Early embryonic Lin$^-$Kit$^+$Flt3$^+$IL7Rα$^+$ immune-restricted progenitors respond to Flt3 ligand and IL7 but develop independently of Flt3 and IL7R signaling

(**A**) Single Lin$^-$Kit$^+$Flt3$^+$IL7Rα$^+$ E11.5 FL cells were analyzed for clonal growth in the absence or presence of IL7 and/or Flt3 ligand (Flt3L) as indicated. Mean ±s.d. number of clones at day 7 (240 cells/group, 4 experiments).
(B) Typical FACS profiles and (**C**) mean ±s.d. frequencies of Lin$^-$Kit$^+$Flt3$^+$IL7Rα$^+$ E11.5 FL cells in WT (**white bar**) and *Flt3l*$^{-/-}$*Il2rg*$^{-/-}$ embryos (**black bar**) (5-6 pooled samples per genotype).

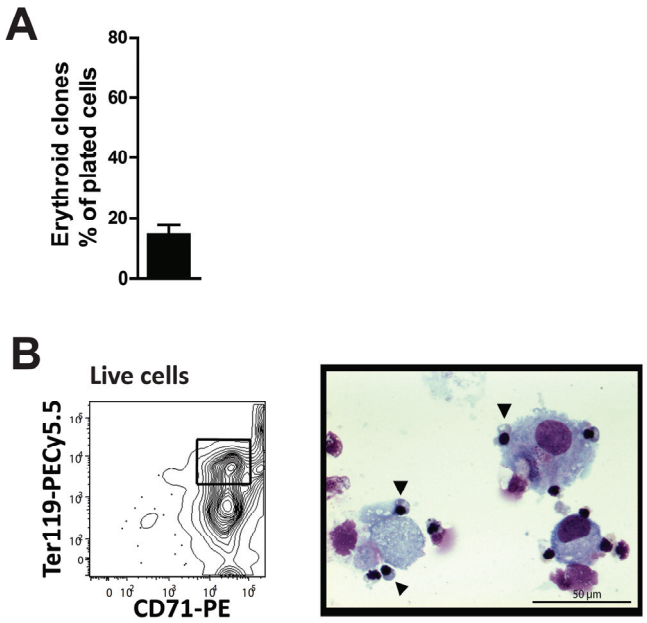

Figure S2 (related to main Figure 2)
Erythroid potential of Lin$^-$Kit$^+$Flt3$^-$IL7Rα$^-$ E11.5 FL cells
(A) Frequency of Lin$^-$Kit$^+$Flt3$^-$IL7Rα$^-$ E11.5 FL progenitors with erythroid potential (clones with Ter119$^+$CD71$^+$ cells and/or positive by morphology) on Op9 stroma under conditions promoting erythroid development. Mean percentage ±s.d. of plated cells (150 cells, 3 experiments).
(B) Representative FACS profile and morphology of erythroid positive well (examples of erythroid cells indicated by arrows).

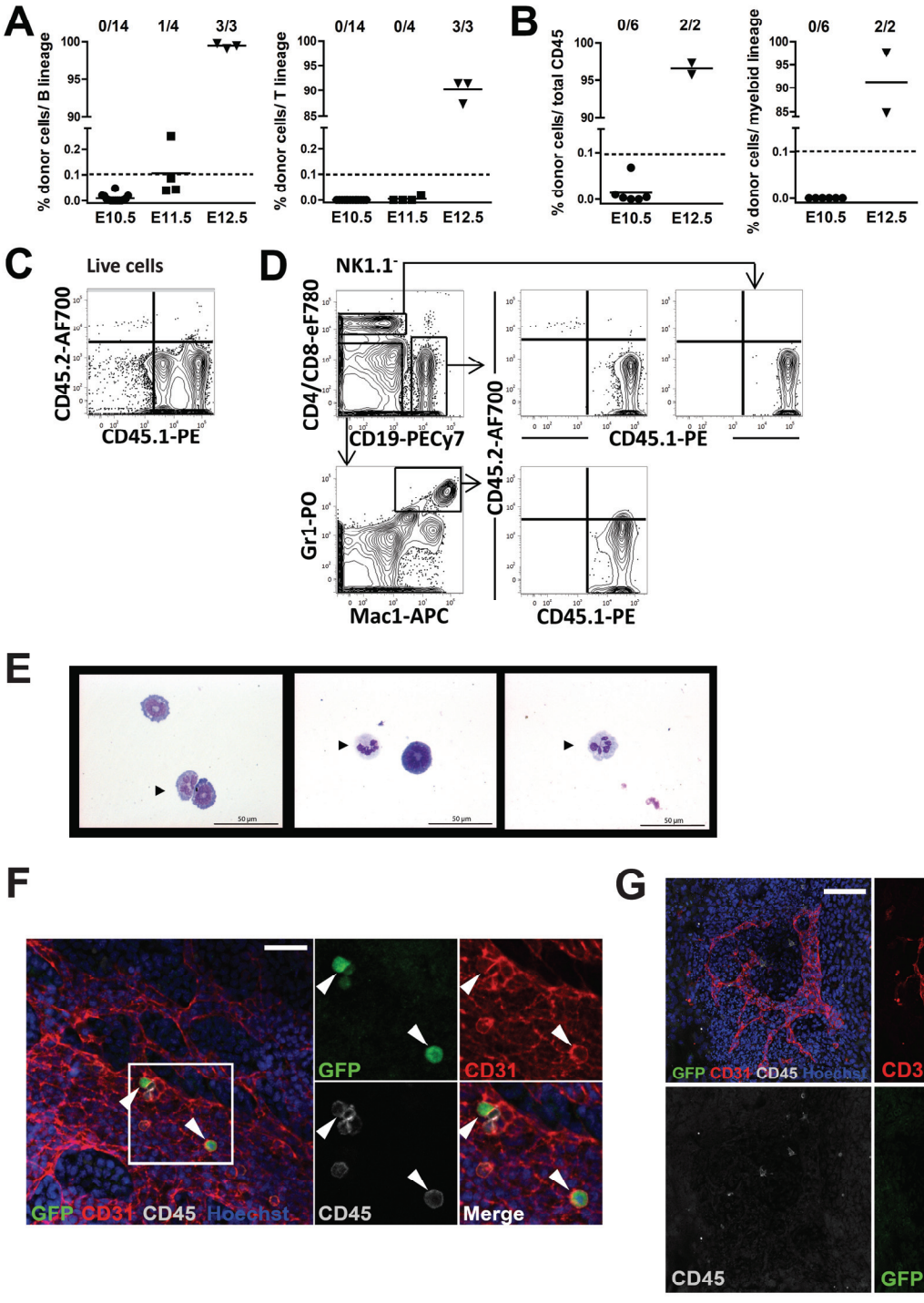
A
0/14
1/4
3/3
% donor cells/ B lineage
E10.5
E11.5
E12.5
0/14
0/4
3/3
% donor cells/ T lineage
B
0/6
2/2
% donor cells/ total CD45
0/6
2/2
% donor cells/ myeloid lineage
C
Live cells
CD45.2-AF700
CD45.1-PE
D
NK1.1-
CD4/CD8-eF780
CD19-PECy7
CD45.2-AF700
CD45.1-PE
Gr1-PO
Mac1-APC
CD45.1-PE
E
50 µm
F
GFP
CD31
GFP CD31 CD45 Hoechst
CD45
Merge
G
GFP CD31 CD45 Hoechst
CD31
CD45
GFP

Figure S3 (related to main Figure 3)

Emergence of lympho-myeloid restricted progenitors precede definitive hematopoietic stem cells in the fetal liver

(A) Unfractionated E10.5 (1 FL/recipient), E11.5 and E12.5 (3-4 FLs/recipient) FL cells were competitively transplanted into lethally irradiated wild-type recipients. Panels show B- and T-cell reconstitution respectively. (Dotted line – detection level (background staining); 0.1% donor contribution). Numbers indicate frequencies of mice reconstituted.

(B) Unfractionated fetal liver (FL) cells from E10.5 (1 FL/recipient) and E12.5 (4-5 FLs/recipient) were transplanted intrafemorally into lethally irradiated wild type recipients. **Left panel** shows total donor and **right panel** myeloid lineage reconstitution. (Dotted line – detection level (background staining); 0.1% donor contribution). Numbers indicate frequencies of mice reconstituted.

(**C-D**) FACS profiles from the mouse reconstituted with the highest level of E11.5 FL derived cells (shown in main **Figure 3A**). (**C**) Total reconstitution and (**D**) contribution of donor (CD45.2) cells to B ($CD19^+$), T ($CD4/CD8^+$) (**upper panels**) and myeloid ($Mac1^+Gr1^+$) (**lower panel**) lineages, respectively.

(**E**) Representative morphology of myeloid cells derived from sorted Lin^-Kit^+*Rag1*$GFP^+IL7R\alpha^+$ E10.5 (30-38 sp) FL cells (granulocytes indicated by arrows).

(**F**) Confocal image of a whole mount immunolabeled YS from E9.5 (23 sp) *Rag1*GFP embryo. Arrows indicate GFP^+ cells in a large vessel that co-express CD31 and CD45. The boxed area is enlarged to show fluorescence in the individual channels. The GFP^+ cell in the top left corner of the boxed area is located within a small $CD45^+$ cluster. Original magnification 250x. Scale bar: 50 μm.

(**G**) *Rag1*GFP PAS were separated from the YS before the establishment of circulation (≤6sp), cultured *ex vivo* and immunolabeled. A representative confocal fluorescence image of an explant-cultured PAS (1 sp) is shown. CD31 and CD45 expressing cells were apparent, but no GFP expression was seen, characteristic of all 7 investigated PAS explants, none of which produced GFP^+ cells within the 48 hours culture time. Original magnification 250x. Tile scan reconstructed image. Scale bar: 200 μm.

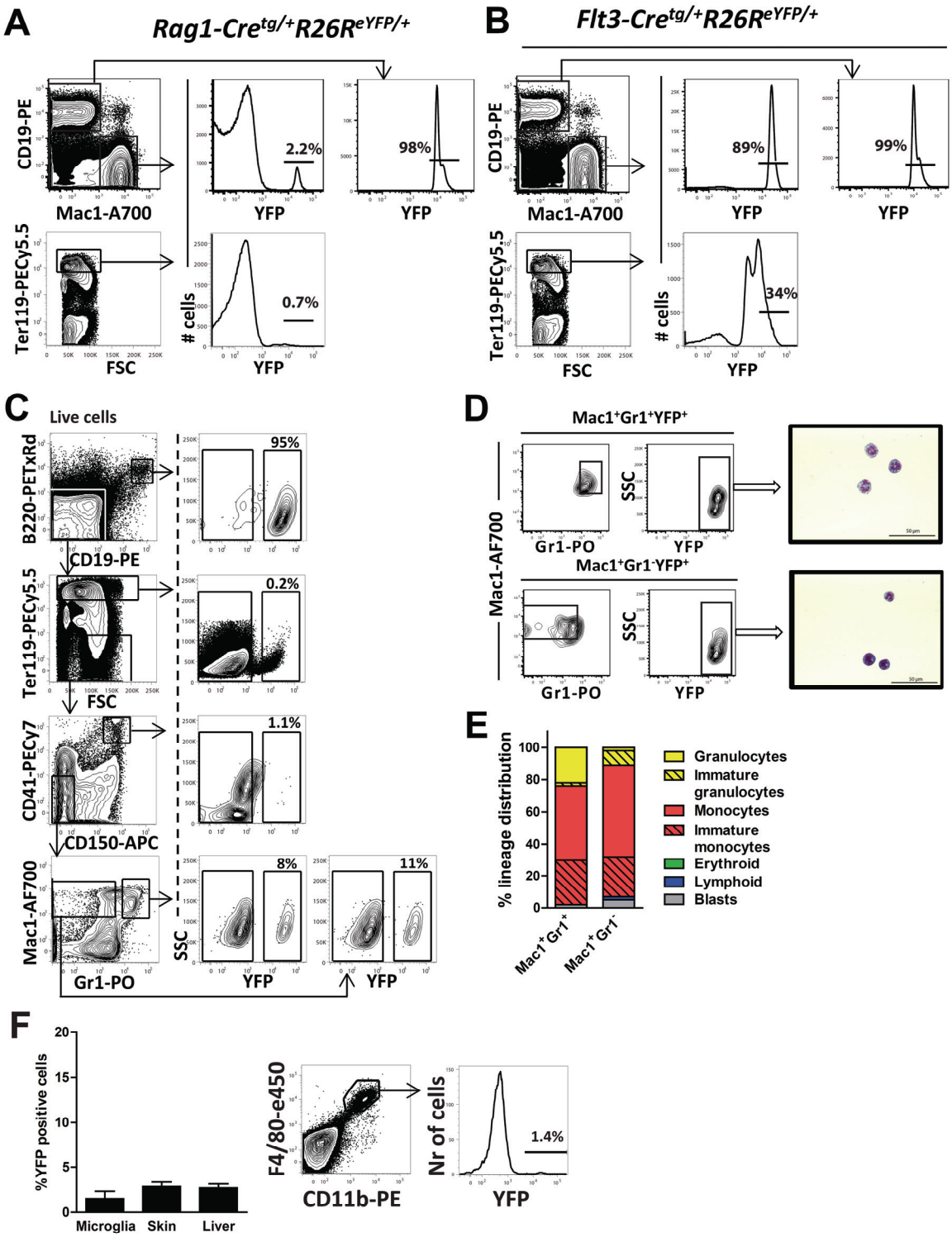
A
Rag1-Cretg/+R26ReYFP/+
CD19-PE
Mac1-A700
2.2%
YFP
98%
YFP
Ter119-PECy5.5
FSC
cells
0.7%
YFP
B
Flt3-Cretg/+R26ReYFP/+
CD19-PE
Mac1-A700
89%
YFP
99%
YFP
Ter119-PECy5.5
FSC
cells
34%
YFP
C
Live cells
B220-PETxRd
CD19-PE
95%
Ter119-PECy5.5
FSC
0.2%
CD41-PECy7
CD150-APC
1.1%
Mac1-AF700
Gr1-PO
SSC
8%
YFP
11%
YFP
D
Mac1+Gr1+YFP+
Mac1-AF700
Gr1-PO
SSC
YFP
Mac1+Gr1-YFP+
Gr1-PO
SSC
YFP
E
% lineage distribution
100
80
60
40
20
0
Granulocytes
Immature granulocytes
Monocytes
Immature monocytes
Erythroid
Lymphoid
Blasts
Mac1+Gr1+
Mac1+Gr1-
F
% YFP positive cells
20
15
10
5
0
Microglia
Skin
Liver
F4/80-e450
CD11b-PE
Nr of cells
1.4%
YFP

Figure S4 (related to main Figure 4)

Lymphoid-primed immune-restricted progenitors contribute to fetal myelopoiesis

Rag1-Cre$^{tg/+}$ (**A**) and *Flt3-Cre*$^{tg/+}$ (**B**) mice were crossed with *R26R*$^{eYFP/eYFP}$ mice and the BM of adult (>8 weeks old) *Cre*$^{tg/+}$*R26R*$^{eYFP/+}$ offspring was analysed by FACS for expression of YFP in different lineages. Results show mean percentages YFP expression in Mac1^{+} (Ter119^{-}CD150^{-}CD41^{-}) myeloid cells and CD19^{+} B cells, (**upper panels**) and Ter119^{+} (CD19^{-}Mac1^{-}Gr1^{-}CD41^{-}CD150^{-}) erythroid cells (**lower panels**). To determine background levels of YFP, CD45.2 experimental samples were mixed with YFP negative BM cells expressing CD45.1 (see **Supplemental Experimental Procedures**). Based on unspecific signal of YFP on CD45.1 cells, unspecific levels were set at 1%.

(**C**) Sorting of myeloid cells from *Rag1-Cre*$^{tg/+}$*R26R*$^{eYFP/+}$ E14.5 FLs. Viable cells were as indicated gated CD19^{-}B220^{-}Ter119^{-}CD41^{-}CD150^{-} and subsequently as Mac1^{+}Gr1^{+} and Mac1^{+}Gr1^{-} populations, and investigated for YFP expression. YFP^{+} and YFP^{-} fractions of Mac1^{+}Gr1^{+} and Mac1^{+}Gr1^{-} FL cells were sorted with indicated gate settings.

(**D**) Purity analysis (**left**) and morphological verification of myeloid cells (**right**) of sorted YFP^{+}Mac1^{+}Gr1^{+} and YFP^{+}Mac1^{+}Gr1^{-} cells.

(**E**) Morphological distribution of cell types within YFP^{-} fraction of Mac1^{+}Gr1^{+} (CD19^{-}B220^{-}Ter119^{-}CD150^{-}CD41^{-}) and Mac1^{+}Gr1^{-} (CD19^{-}B220^{-}Ter119^{-}CD150^{-}CD41^{-}) cells sorted from *Rag1-Cre*$^{tg/+}$*R26R*$^{eYFP/+}$ E14.5 FLs. Mean percentages from 2 experiments.

(**F**) Brain, skin and liver tissue macrophages from E14.5 *Rag1-Cre*$^{tg/+}$*R26R*$^{eYFP/+}$ embryos were investigated for YFP expression. Microglia : CD45^{low}CD11b^{+}F4/80^{+} ; Skin and liver : CD45^{+} CD11b^{+}F4/80^{bright} . Mean percentages YFP expression ±s.d. (7 embryos). Representative FACS profile of microglia gating is shown to the right.

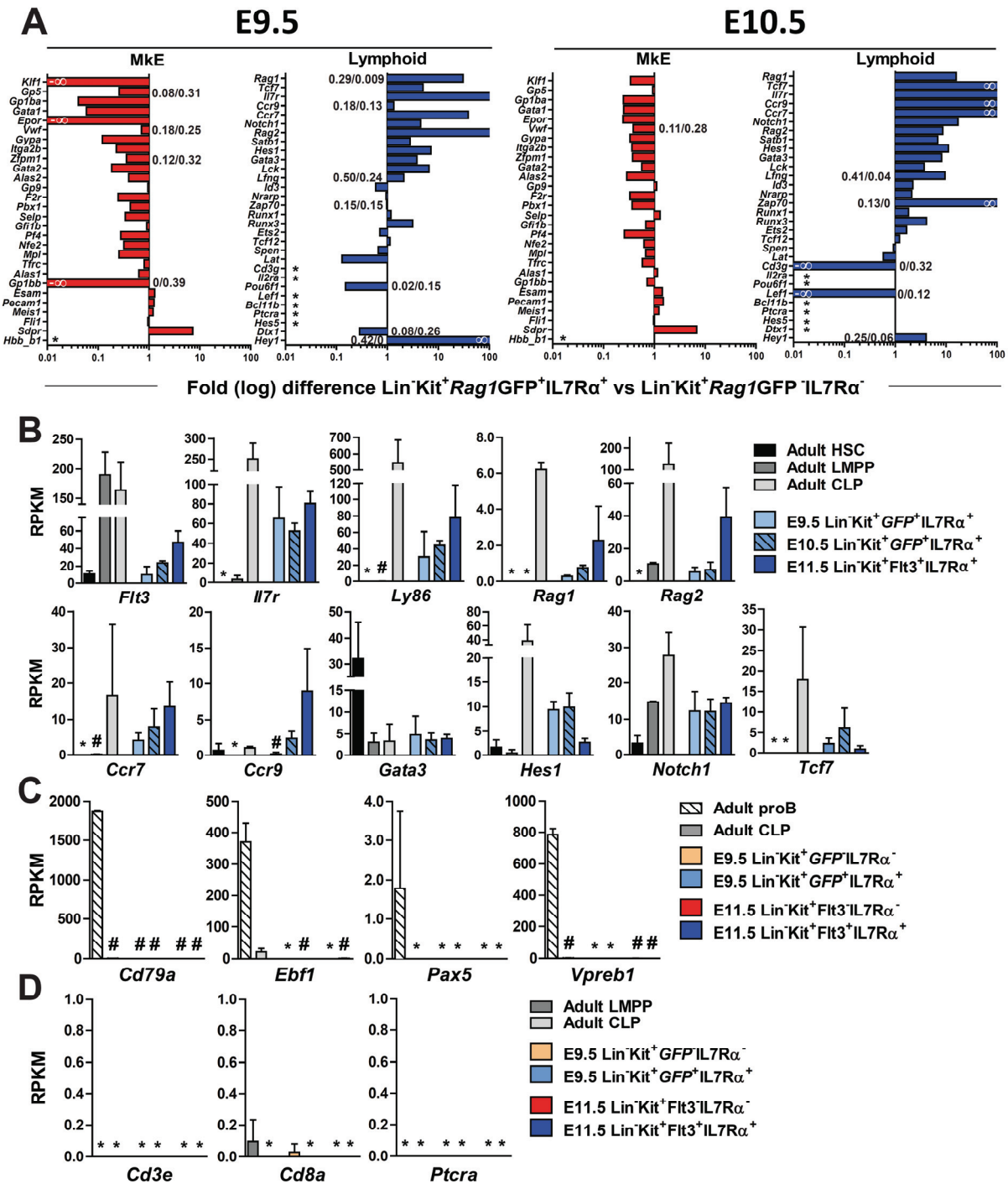
A
E9.5
E10.5
MkE
Lymphoid
0.08/0.31
0.18/0.25
0.12/0.32
0/0.39
0.29/0.009
0.18/0.13
0.50/0.24
0.15/0.15
0.02/0.15
0.08/0.26
0.42/0
0.11/0.28
0.41/0.04
0.13/0
0/0.32
0/0.12
0.25/0.06
Fold (log) difference Lin-Kit+Rag1GFP+IL7Rα+ vs Lin-Kit+Rag1GFP-IL7Rα-
B
RPKM
Flt3
Il7r
Ly86
Rag1
Rag2
Ccr7
Ccr9
Gata3
Hes1
Notch1
Tcf7
Adult HSC
Adult LMPP
Adult CLP
E9.5 Lin-Kit+GFP+IL7Rα+
E10.5 Lin-Kit+GFP+IL7Rα+
E11.5 Lin-Kit+Flt3+IL7Rα+
C
RPKM
Cd79a
Ebf1
Pax5
Vpreb1
Adult proB
Adult CLP
E9.5 Lin-Kit+GFP-IL7Rα-
E9.5 Lin-Kit+GFP+IL7Rα+
E11.5 Lin-Kit+Flt3-IL7Rα-
E11.5 Lin-Kit+Flt3+IL7Rα+
D
RPKM
Cd3e
Cd8a
Ptcra
Adult LMPP
Adult CLP
E9.5 Lin-Kit+GFP-IL7Rα-
E9.5 Lin-Kit+GFP+IL7Rα+
E11.5 Lin-Kit+Flt3-IL7Rα-
E11.5 Lin-Kit+Flt3+IL7Rα+

Figure S5 (related to main Figures 5 and 6)

Upregulation of lymphoid genes initiates in Lin$^-$Kit$^+$*Rag1*GFP$^+$IL7Rα$^+$ E9.5 YS progenitors

(A) Lin$^-$Kit$^+$*Rag1*GFP$^+$IL7Rα$^+$ and Lin$^-$Kit$^+$*Rag1*GFP$^-$IL7Rα$^-$ E9.5 YS and E10.5 FL cells were subjected to global RNA sequencing and analysed for differences in MkE and lymphoid gene expression of previously published lineage-associated programs (Luc et al., 2012). Mean fold differences (of 3 replicates) in RPKM (=reads per kilobase of exon model per million mapped reads) expression values of the specified genes in Lin$^-$Kit$^+$*Rag1*GFP$^+$IL7Rα$^+$ relative to Lin$^-$Kit$^+$*Rag1*GFP$^-$IL7Rα$^-$ cells shown on a $\log_{10}$ scale. *: RPKM $\leq$ 0.05 for both cell populations. For genes with expression $\leq$ 0.5 RPKM for both cell populations, specific values are indicated next to bars. ∞: infinity.

(B) Expression of lymphoid genes in immune-restricted progenitors based on RNA sequencing at E9.5 YS, E10.5 FL and E11.5 FL as compared to adult HSCs, LMPPs and CLPs. Mean RPKM ±s.d. of 2-3 replicates. *: not detected, #: expressed but at too low level to be visualized on the applied scale.

(**C-D**) Absence of B-cell (**C**) and T-cell (**D**) specific gene expression in E9.5 YS Lin$^-$Kit$^+$*Rag1*GFP$^+$IL7Rα$^+$ and Lin-Kit$^+$*Rag1*GFP$^-$IL7Rα$^-$ and E11.5 FL Lin$^-$Kit$^+$Flt3$^+$IL7Rα$^+$ and Lin$^-$Kit$^+$Flt3$^-$IL7Rα$^-$ progenitors. Mean RPKM ±s.d. of 2-3 replicates.

*: not detected, #: expressed but at too low level to be visualized on the applied scale.

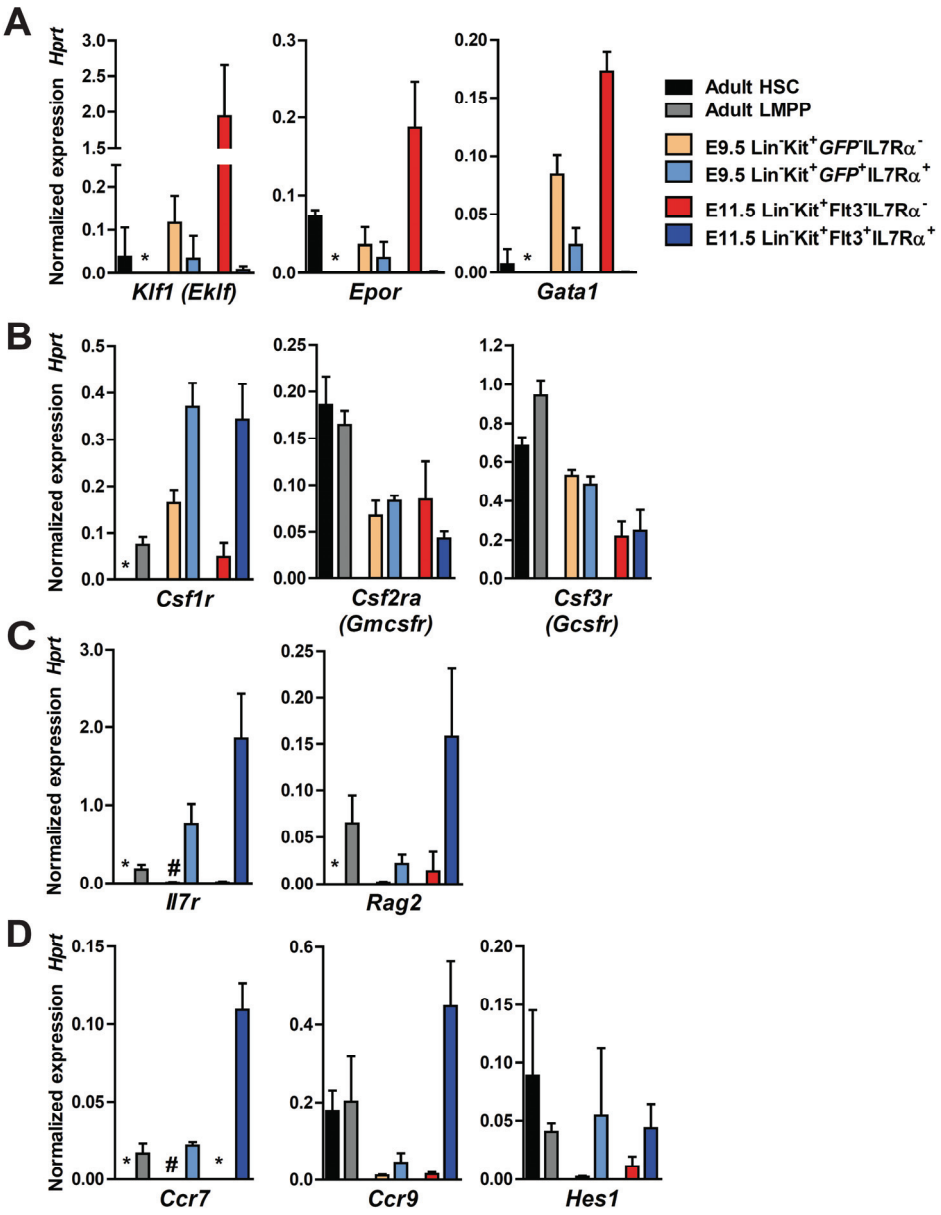

Figure S6 (related to main Figures 5 and 6)

Validation of RNA sequencing data with quantitative PCR

Lin$^-$Kit$^+$*Rag1*GFP$^+$IL7Rα$^+$ (and Lin$^-$Kit$^+$*Rag1*GFP$^-$IL7Rα$^-$) E9.5 YS and Lin$^-$Kit$^+$Flt3$^+$IL7Rα$^+$ (and Lin$^-$Kit$^+$Flt3$^-$IL7Rα$^-$) E11.5 FL cells were subjected to quantitative gene expression analysis and compared to adult HSCs and LMPPs. (**A**) MkE (**B**) GM (**C**) lymphoid and (**D**) thymus-seeding progenitor related genes. Mean ±s.d. gene expression values normalized to *Hprt* (3-5 experiments, 25 cells/sample). *: not detected, #: expressed but at too low level to be visualized on the applied scale.

Table S1 (related to main Figures 5 and 6)

Commonly upregulated genes in E9.5 YS and E11.5 FL immune-restricted progenitors.

Gene	Protein	Function (Ref)
2010001M09Rik	RIKEN cDNA 2010001M09 gene (Mzb1 protein)	Luminal ER protein, regulation of innate-like B-cell functions (Flach et al., 2010)
Abcg3	ATP-binding cassette, sub-family G, member 3	Efflux transport of cholesterol (Kusuhara and Sugiyama, 2007)
Alcam	Activated leukocyte cell adhesion molecule	Cell adhesion, migration (Swart, 2002)
Bfsp2	Beaded filament structural protein 2, phakinin	Cytoskeletal protein (Perng and Quinlan, 2005)
Calcrl	Calcitonin receptor-like	Signaling, G protein-coupled receptor (Harzenetter et al., 2002)
Ccnd2	Cyclin D2	Regulation of cell cycle (Chiles, 2004)
Cd27	CD27 antigen	Immune signaling (binds CD70) (Denoeud and Moser, 2011)
Cd33	CD33 antigen	Adhesion receptor (sialic acid-dependent) (Brinkman-Van der Linden et al., 2003)
Cd7	CD7 antigen	Immune signaling (Yoshikawa et al., 1993)
Cdh17	Cadherin 17	Cell adhesion and signaling (Ohnishi et al., 2005)
Clec12a	C-type lectin domain family 12, member a	Cell adhesion and signaling in dendritic cells (Pyz et al., 2008)
Ctnnd2	Catenin (cadherin associated protein), delta 2	Cell adhesion and motility in neural cells (armadillo/β-catenin superfamily) (Lu, 2010)
Cybb	Cytochrome b-245, beta polypeptide	Microbicidal oxidase system (El-Benna et al., 2010)
Dpysl2	Dihydropyrimidinase-like 2	Signaling, cytoskeletal remodeling (Chae et al., 2009)
Dusp6	Dual specificity phosphatase 6	Dual-specificity phosphatase, MAPK/ERK signaling (Bermudez et al., 2010)
Emcn	Endomucin	Cell adhesion and signaling in endothelial cells (Kinoshita et al., 2001)
Entpd1	Ectonucleoside triphosphate diphosphohydrolase 1 (Cd39)	Transmembrane protein, ATP and ADP hydrolysis (Sitkovsky et al., 2008)
Ets1	E26 avian leukemia oncogene 1, 5' domain	Transcriptional coactivator, regulated by Sp100 (Dittmer, 2003)
Fgd2	FYVE, RhoGEF and PH domain containing 2	Signaling, expressed in antigen presenting cells (Huber et al., 2008)
Flt3	FMS-like tyrosine kinase 3	Immune signaling, cytokine receptor tyrosine kinase (Rosnet et al., 1996)
Gem	GTP binding protein (overexpressed in skeletal muscle)	Signaling (Maguire et al., 1994)
Gimap6	GTPase, IMAP family member 6	GTPase, IMAP family member, cell signaling, T cell survival (Nitta and Takahama, 2007)
Gimap7	GTPase, IMAP family member 7	GTPase, IMAP family member, cell signaling , T cell survival (Nitta and Takahama, 2007)
Gngt2	Guanine nucleotide binding protein (G protein), gamma transducing 2	Signaling, G protein coupled receptor (Ong et al., 1997)
Gpr171	G protein-coupled receptor 171	Signaling, purinergic G protein-coupled receptor (uncharacterised)
Gpr65	G-protein coupled receptor 65	Signaling, pH-sensing G protein-coupled receptor (Onozawa et al., 2011)
Gsn	Gelsolin	Cytoskeletal protein (Silacci et al., 2004)
Hmgn3	High mobility group nucleosomal binding domain 3	Nucleosome binding protein (West et al., 2001)
Ifi203	Interferon activated gene 203	Cell growth and differentiation, interferon inducible (Gariglio et al., 2011)
Ifitm3	Interferon induced transmembrane protein 3	Cell migration and homing in the embryo (Tanaka et al., 2005) and viral resistance (Everitt et al., 2012)
Ift57	Intraflagellar transport 57 homolog	Trasncriptional coactivator, pro-apoptotic (Datta et al., 2011)
Il1r2	Interleukin 1 receptor, type II	Immune signaling, IL-1inhibitory decoy receptor (Tran et al., 2009; Wang et al., 2008)
Il7r	Interleukin 7 receptor alpha chain	Cytokine receptor, immune signaling (Kallies, 2008)
Klrd1	Killer cell lectin-like receptor, subfamily D, member 1	Immune signaling, receptor of MHC class I antigen E with peptide (Borrego et al., 2005)
Lax1	Lymphocyte transmembrane adaptor 1	Immune signaling, transmembrane adaptor protein (Fuller and Zhang, 2009)
Lsp1	Lymphocyte specific 1	Lymphoid F-actin bundling cytoskeletal protein (Jongstra-

		Bilen and Jongstra, 2006)
Ly86	Lymphocyte antigen 86	Lymphoid extracellular protein (Gorczynski et al., 2006)
Marcks	Myristoylated alanine rich protein kinase C substrate	Cytoskeletal protein (Rombouts et al., 2012)
Mn1	Meningioma 1	Transcriptional coactivator, regulatory T cell development (Meester-Smoor et al., 2008)
Mndal	Myeloid nuclear differentiation antigen like	Cell growth and differentiation, interferon inducible (Gariglio et al., 2011)
Mycn	v-myc myelocytomatosis viral related oncogene, neuroblastoma derived	Transcriptional coactivator (Westermark et al., 2011)
Napsa	Napsin A aspartic peptidase	Aspartic peptidase (Schauer-Vukasinovic et al., 2000)
Notch1	Notch gene homolog 1 (Drosophila)	Notch receptor, immune signaling (Rothenberg, 2011)
P2ry12	Purinergic receptor P2Y, G-protein coupled 12	Signaling, purinergic G protein-coupled receptor (Rossi et al., 2007)
P2ry14	Purinergic receptor P2Y, G-protein coupled, 14	Signaling, purinergic G protein-coupled receptor (Lee et al., 2003; Rossi et al., 2007)
Plk2	Polo-like kinase 2	Regulation of cell cycle (van de Weerdt and Medema, 2006)
Ppp1r16b	Protein phosphatase 1, regulatory (inhibitor) subunit 16B	Cell signaling (Magdaleno et al., 2002)
Prss2	Protease, serine, 2	Serine protease (Carabana et al., 2011)
Psmb8	Proteasome subunit, beta type 8 (large multifunctional peptidase 7)	Immunoproteasome, antigen cleavage (Atkinson et al., 2012)
Psmb9	Proteasome (prosome, macropain) subunit, beta type 9	Immunoproteasome, antigen cleavage (Atkinson et al., 2012)
Ptprc	Protein tyrosine phosphatase, receptor type, C	Immune signaling, protein phosphatase (Clement, 1992)
Pygm	Muscle glycogen phosphorylase	Glycogen metabolism (Andreu et al., 2007)
Rag2	Recombination activating gene 2	Immunoglobulin V(D)J rearrangement (Schatz and Ji, 2011)
Rgs1	Regulator of G-protein signaling 1	Immune signaling from G protein-coupled receptors (Moratz et al., 2000)
Runx2	Runt related transcription factor 2	Transcriptional coactivator (de Bruijn and Speck, 2004)
Serpinb1a	Serine/cysteine peptidase inhibitor, clade B, member 1a	Serine protease inhibitor (Benarafa et al., 2011; Painter et al., 2011)
Sesn1	Sestrin 1	Protection from oxidative stress (Budanov, 2011)
Snn	Stannin	Regulation of cell cycle (Reese et al., 2006)
Sp100	Nuclear antigen Sp100	Nuclear Protein, interferon inducible (Szostecki et al., 1990)
St8sia4	ST8 alpha-N-acetyl-neuraminide alpha-2,8-sialyltransferase 4	Polysialation of membrane proteins, role in T-cell proliferation (Angata et al., 2004)
Stc1	Stanniocalcin 1	Secreted protein, oxidative stress response, calcium/phosphate homeostasis (Yeung et al., 2012)
Tifa	TRAF-interacting protein with forkhead-associated domain	Immune signaling, adaptor protein (Ea et al., 2004)
Tnip3	TNFAIP3 interacting protein 3	Immune signaling (Verstrepen et al., 2009)
Tnni2	Troponin I, skeletal, fast 2	Muscle contraction (Kee and Hardeman, 2008)
Tsc22d1	TSC22 domain family, member 1	Signaling (Nakamura et al., 2012)
Tshz3	Teashirt zinc finger family member 3	Muscle development (Faralli et al., 2011)
Zcchc18	Zinc finger, CCHC domain containing 18	Zinc finger domain containing protein (uncharacterized)

Table shows information regarding encoded proteins and their known functions (including relevant references) of genes significantly ($p<0.1$) upregulated in both E9.5 YS Lin^-Kit^+*Rag1*$GFP^+IL7R\alpha^+$ and E11.5 FL $Lin^-Kit^+Flt3^+IL7R\alpha^+$ progenitors when compared to E9.5 YS Lin^-Kit^+*Rag1*$GFP^-IL7R\alpha^-$ and E11.5 FL $Lin^-Kit^+Flt3^-IL7R\alpha^-$ progenitors, respectively (3 replicates/cell population). Exact p-values and fold upregulation for each gene is included in **Tables S2** and **S3.**

Table S2 (related to main Figures 5 and 6)

Upregulated genes in E9.5 YS Lin$^-$Kit$^+$Rag1GFP$^+$IL7Rα$^+$ immune-restricted progenitors.

Gene	Fold change (DESeq)	Adjusted P-value (DESeq)
Il7r	241.2262	7.53E-15
Mndal	101.2168	1.17E-13
Gpr171	7.91427	1.69E-13
Lsp1	17.29018	5.22E-13
Flt3	116.8016	5.51E-13
Il1r2	14.1349	5.87E-09
Ifitm1	10.8593	5.87E-09
Gimap6	5.868762	5.87E-09
Gimap7	Inf	2.50E-08
Rag2	320.3892	3.02E-08
Serpinb8	51.44116	1.56E-07
P2ry12	Inf	1.56E-07
Runx2	20.11023	2.39E-07
Bcl11a	5.348086	2.39E-07
Cd27	17.29347	2.83E-07
Napsa	18.69008	5.86E-07
Mn1	10.94985	8.79E-07
Lax1	9.121819	3.76E-06
2010001M09Rik	16.31282	3.80E-06
Cdh17	29.7894	4.92E-06
Klrd1	63.28746	1.98E-05
Bfsp2	27.31353	2.18E-05
Psmb9	7.35932	6.28E-05
Cd7	Inf	0.000115
Tnni2	6.846342	0.000156
Ifitm3	5.848924	0.000352
Prss2	37.39997	0.000595
AI662270	3.490624	0.00063
Stc1	512.995	0.000641
Cybb	65.84472	0.000641
Sfxn3	62.33848	0.000641
Chst2	Inf	0.000641
Psmb8	3.428959	0.000815
Tifa	3.688451	0.001038
Notch1	4.43373	0.001204
Rgs1	3.797913	0.001418
Gngt2	7.911953	0.001553
Dusp6	3.5811	0.001894
Ets1	3.63082	0.003448
Gem	4.535833	0.00356
Cd33	10.91258	0.004206
Ly86	8.729357	0.006354
Ppp1r16b	11.19762	0.006791
Emcn	7.46899	0.007457
Tshz3	19.668	0.007826
Ptprc	3.451179	0.007826
Tnfsf10	11.49241	0.00819
Klhl4	14.12903	0.008236
Lair1	16.5607	0.009716
Epsti1	75.68386	0.010557
Mr1	Inf	0.010557
Ift57	6.19188	0.01092
Sp100	7.415384	0.011712
Clec12a	2.921238	0.012761
Serpinb1a	2.684283	0.015587
Dpysl2	2.758877	0.019207
Calcrl	3.217305	0.020144
Klhl24	3.402242	0.020753
Abcg3	7.258606	0.020768
Ctnnd2	54.39778	0.021266
Btg1	3.1069	0.021689
Rb1	5.949324	0.021833
Gpr65	3.756539	0.022016
Arntl	3.179337	0.022777
Tnfrsf13c	Inf	0.022802
Serpinb6b	5.61891	0.025765
Mycn	4.1764	0.028503
Ifi203	Inf	0.028605
Rhoh	2.934116	0.034056
Ddx60	15.26211	0.034823
Snn	12.41512	0.039259
P2ry14	3.744636	0.039386
St8sia4	4.188037	0.042453
Sesn1	2.791182	0.045658
Alcam	7.105028	0.049296
Tnip3	5.193218	0.057478
Entpd1	5.332876	0.068333
Ptprs	3.009405	0.068333
Mecom	51.21089	0.069215
Gsn	9.927191	0.070063
Plk2	5.521084	0.073039
Marcks	6.533277	0.07544
Hmgn3	3.237165	0.07613
Tsc22d1	2.689993	0.08112
Ccnd2	2.491469	0.089216
Pygm	13.03616	0.089917
Fgd2	6.057014	0.090114
Zcchc18	16.86993	0.094229
Plekha2	2.764604	0.097134

List of genes significantly (adjusted p-value<0.1) upregulated in E9.5 YS Lin$^-$Kit$^+$*Rag1*GFP$^+$IL7Rα$^+$ progenitors when compared to Lin$^-$Kit$^+$*Rag1*GFP$^-$IL7Rα$^-$ progenitors, ranked by increasing p-values, adjusted for multiple testing with the Benjamini-Hochberg procedure, as determined by the DESeq package (version 1.6.1). Also shown is the mean fold upregulation based on 3 replicates. Inf: infinity, reflecting undetectable expression in Lin$^-$Kit$^+$*Rag1*GFP$^-$IL7Rα$^-$ cells.

Table S3 (related to main Figures 5 and 6)
Upregulated genes in E11.5 FL Lin$^-$Kit$^+$Flt3$^+$IL7Rα$^+$ immune-restricted progenitors.

Gene	Fold change (DESeq)	Adjusted p-value (DESeq)
Mndal	1241.828	1.02E-23
2010001M09Rik	Inf	2.05E-16
Lsp1	35.02766	9.52E-14
Gpr171	9.826083	6.42E-13
Mn1	45.62222	7.85E-13
Notch1	28.70085	9.39E-13
Ccl3	60.8317	1.14E-11
Flt3	99.22809	4.11E-11
Il12a	8.270356	1.01E-10
Il7r	118.7861	1.54E-10
Dusp6	11.16424	2.25E-10
Tmem173	9.497857	2.25E-10
Gimap6	7.510334	4.23E-10
Rgs2	7.214871	8.55E-10
Ifi203	278.4957	2.48E-09
Gimap4	14.06201	1.52E-08
Lax1	15.83442	2.09E-08
Runx2	24.85105	5.60E-08
Clec12a	13.1914	7.86E-08
Tnni2	19.38705	1.02E-07
Cdh17	90.71277	2.50E-07
H2-DMa	10.77154	4.56E-07
Cd27	17.3811	5.12E-07
Cd93	4.412292	8.74E-07
Rgs1	8.15945	1.28E-06
Ets1	8.407611	2.25E-06
Ctss	78.71546	3.03E-06
Il1r2	12.87149	4.94E-06
Efna5	53.64187	5.25E-06
Gm5111	13.71904	9.62E-06
Blnk	Inf	9.62E-06
Gimap7	28.91417	1.02E-05
Ly6a	25.01933	1.44E-05
Calcrl	4.93352	1.90E-05
Tlr7	231.2857	2.31E-05
Enc1	7.654327	2.31E-05
Anxa1	5.036684	2.31E-05
Cd34	3.916183	2.31E-05
Ctnnd2	Inf	2.31E-05
Ly86	42.26483	2.35E-05
Mef2c	3.896631	2.47E-05
Ncf1	10.45594	2.55E-05
Cox6a2	106.5839	2.64E-05
Ppp1r16b	48.75928	2.77E-05
Ifitm3	7.527046	2.96E-05
Ddx4	9.348242	3.63E-05
H2afy	3.609173	3.76E-05
H2-Ob	23.29679	5.02E-05
Arhgef3	7.782846	5.36E-05
Dse	41.06779	0.000116
Napsa	13.90376	0.000117
P2ry14	5.736251	0.00012
Hlf	4.962859	0.00012
Gpr65	6.583818	0.000144
Irf8	16.50056	0.000159
Rasgrp3	47.29354	0.000165
Cd33	29.47153	0.000165
Rag2	26.22804	0.000199
Itgam	11.02558	0.000213
St8sia1	76.23944	0.000232
Gem	6.349692	0.000263
Prss2	Inf	0.000321
Ifi27l1	7.193487	0.000391
Il18	Inf	0.000443
Gbp2	69.47674	0.000468
Ptprc	3.689159	0.00047
Cybb	111.4735	0.000476
Pkib	15.30674	0.00065
Cobll1	141.8728	0.000705
Cav2	30.75709	0.000705
Mycn	5.273974	0.000705
Tspan2	7.683997	0.000727
Entpd1	18.49583	0.000787
Psmb8	5.357475	0.000844
Il16	4.2477	0.000849
Emcn	6.630647	0.000861
Serpinb1a	3.295534	0.000968
Cfp	36.95467	0.001005
Lpar6	3.735764	0.001031
Ednrb	12.81301	0.001074
Slc18a1	46.0342	0.001483
Stat4	3.595441	0.001501
Ugt1a7c	19.65313	0.001632
Mgst2	8.118649	0.001632
Eltd1	2.717934	0.001632
Cd7	70.05544	0.001678
P2ry12	143.8188	0.002048
Lcp1	2.803945	0.002159
Rnd3	12.19681	0.002518
Ecscr	6.230575	0.002702
Satb1	7.627213	0.002717
Zfhx3	3.75635	0.002732
Sp100	20.5688	0.002898
Ccl4	80.88612	0.003367
Gpr18	Inf	0.003601
Stc1	Inf	0.003923
Hpgd	6.656653	0.003943
Dusp22	40.33862	0.004109
Irf5	12.95861	0.004137
9030619P08Rik	8.221757	0.004614
Fcrl1	36.61472	0.005134
Rnf13	3.012423	0.005697
Cd200	28.78006	0.005743
Tmem154	10.2957	0.005743
Egfl7	4.802601	0.005743
Sdc4	Inf	0.005743
Klrd1	36.18403	0.005783
Tox	6.217454	0.00591

Ctr9	3.269104	0.006232
Rag1	Inf	0.00625
Fam107b	2.707895	0.007032
Slc39a6	4.094298	0.007447
Cd69	6.042798	0.008502
Hmga2	3.446395	0.008786
Cd53	3.21867	0.009001
Gcnt2	2.867911	0.009905
Tcf7l2	6.129858	0.010238
Abcg3	9.228849	0.010574
Marcks	10.20704	0.010652
Il1r1	5.277979	0.010652
Gngt2	7.813134	0.010699
Bex6	5.221945	0.010712
Gm11428	27.90881	0.010758
Tnip3	5.139042	0.010758
Zcchc18	Inf	0.010758
Il21r	7.32458	0.0111
Elmo1	2.491034	0.011911
Snn	19.85931	0.012126
Gm4759	Inf	0.012126
Ccr2	31.49859	0.014404
Fgf10	52.0992	0.014695
Tsc22d1	3.118333	0.014742
Dpysl2	2.519198	0.016381
Map3k1	2.648771	0.017557
Tyrobp	4.907725	0.018869
P2ry13	23.27775	0.019322
Hpgds	4.776365	0.019322
Mier3	2.494718	0.019322
Ablim1	11.5726	0.021246
Ift57	5.426901	0.021968
Zfp36	2.917959	0.02212
Hoxa10	21.90863	0.022685
Cd24a	3.241845	0.023521
Tpm4	3.566642	0.023611
Csf1r	10.91952	0.024379
Gimap9	2.882853	0.025127
Tcf4	2.863916	0.025127
Pygm	19.65968	0.025817
St8sia4	4.107967	0.025837
Ptger2	13.17627	0.026478
Cd86	6.812727	0.026478
Slc9a9	25.09233	0.027903
Abi3	10.16178	0.028765
Tifab	9.248642	0.028765
Nfil3	23.58759	0.032438
Pld4	55.73325	0.033535
Bfsp2	7.179956	0.034129
Pstpip1	5.508383	0.034755
Pde2a	11.86481	0.035391
Plk2	6.287162	0.035852
Cd82	7.008936	0.036471
Paqr5	Inf	0.036716
Camk2d	7.403905	0.037668
Smad7	14.39568	0.03778
Alcam	21.46427	0.03845
Bcl2	5.635148	0.038634
Tshz3	13.60397	0.039518
Ppp3ca	2.810184	0.040468
Coro2a	2.524507	0.042932
Capsl	7.514237	0.043212
Arl11	5.246834	0.043599
Fgd2	8.669693	0.047125
Ccnd1	6.532847	0.047917
Icos	12.95081	0.053812
Psmb9	5.146873	0.054119
Sesn1	2.97734	0.054119
Rassf5	3.090739	0.054123
Tbc1d10c	4.182288	0.057191
Tifa	2.575167	0.057274
Tes	2.497395	0.057274
Cd47	2.422942	0.058666
Usp22	2.292343	0.058666
Sema3d	Inf	0.059662
Ccnd2	2.309944	0.059916
Gsn	10.07031	0.062653
Ebi3	4.465292	0.063565
Afap1l1	3.413133	0.064338
Tet1	2.874152	0.06798
Kif17	Inf	0.068286
Sdpr	32.63225	0.072787
Gapt	13.78965	0.07591
Sqrdl	Inf	0.078947
Lat2	3.970846	0.080122
Ebf1	Inf	0.081257
Dhrs3	4.94913	0.081789
Unc93b1	6.000192	0.091561
Abr	6.317259	0.092179
Spata13	3.558774	0.095732
Igtp	4.195358	0.09821
Hoxa9	17.9201	0.09844
Hmgn3	3.312363	0.098577

List of genes significantly (adjusted p-value<0.1) upregulated in E11.5 FL $Lin^{-}Kit^{+}Flt3^{+}IL7R\alpha^{+}$ progenitors when compared to $Lin^{-}Kit^{+}Flt3^{-}IL7R\alpha^{-}$ progenitors, ranked by increasing p-values, adjusted for multiple testing with the Benjamini-Hochberg procedure, as determined by the DESeq package (version 1.6.1). Also shown is the mean fold upregulation based on 3 replicates Inf: infinity, reflecting undetectable expression in $Lin^{-}Kit^{+}Flt3^{-}IL7R\alpha^{-}$ cells.

SUPPLEMENTAL EXPERIMENTAL PROCEDURES

Animals and cell preparations

Mouse strains used; C57BL/6 (CD45.1 or CD45.2), *Rag1*-GFP (Kuwata et al., 1999), (Importantly, to exclude maternal/placental cell contamination, *Rag1*-GFP was always inherited from the male parent to ensure that GFP expressing cells are solely embryo-derived.) *Flt3l*$^{-/-}$*Il2rg*$^{-/-}$ (Sitnicka et al., 2003)(Sitnicka et al., 2007). *Flt3-Cre*$^{tg/+}$ and *Rag1-Cre*$^{tg/+}$ mice were mated with Rosa26 (R26R)$^{eYFP/eYFP}$ mice and have previously been described (Benz et al., 2008; McCormack et al., 2003; Srinivas et al., 2001). All mouse strains were backcrossed to a C57BL/6 genetic background. Before E11, embryos were staged by counting somite pairs and dissected as previously described (Bee et al., 2010). YS was dissected without vitelline and umbilical cord and treated with collagenase (type 1, Sigma; final concentration 0.12%) for 10 min, 37°C. FL was mechanically disrupted with a syringe (E11.5) or treated with collagenase (E10.5) as above. Cell suspensions from E8.5 embryos were obtained by collagenase treatment of whole concepti (YS, allantois and embryo proper combined, without the ectoplacental cone). E14.5 thymuses were dissected and single cell suspension made with a syringe. Cells were counted with the Sysmex (KX-21N) Hematology analyser or manually counted in a Neubauer chamber with trypan blue.

Tissue macrophages

For analysis of tissue macrophages, single cell suspensions of dissected tissues from E14.5 *Rag1-Cre*$^{tg/+}$*R26R*$^{eYFP/+}$ embryos were generated by 30min incubation at 37ºC in PBS with 0.5mg/ml Collagenase D (Roche), 2.4mg/ml Dispase (Invitrogen), 100U/mL Deoxyribonuclease I (DNAse I, Sigma) and 3% fetal bovine serum (Invitrogen) followed by light mechanical disruption. The following antibodies were used to stain the tissues for flow cytometry (BD Canto II); FcgRIII/II (Fc-block, 2.4G2), CD45.2 APC-Cy7 (104), F4/80–A450 (BM8), CD11b-PE (M1/70), Gr1-APC (RB6-8C5); c-Kit-PECy7 (2B8). Microglia were defined as CD45^{low}CD11b^{+}F4/80^{+} and tissue macrophages in skin and liver as CD45^{+}CD11b^{+}F4/80^{bright}.

Fluorescence Activated Cell Sorting (FACS)

Adult HSC and LMPP cell preparations were enriched for CD117 expression by MACS bead separation with anti-CD117 (c-kit) immunomagnetic beads (Miltenyi Biotec) in cell sorting experiments. Antibodies used to stain embryonic progenitors, bone marrow progenitors, *Rag1*-cre fate mapping and staining of peripheral blood are listed in the **Tables below**. All cell sorting experiments were performed on a BD FACSAriaI or II cell sorter and all FACS analyses on a BD LSRII (see **Table below** for configuration of instruments). Subsequent data analyses were performed with the FlowJo analysis software (TreeStarInc).

Antibody panels used for characterization of embryonic progenitors and Rag1-Cre fate mapping

Antibody-conjugate	Clone	Supplier	Application
Ter119-APC or TER119-PECy5	TER119	eBioscience, Biolegend	embryonic progenitors
Gr1-APC	RB6-8C5	BD, Biolegend	embryonic progenitors
F4/80-APC	BM8	Invitrogen	embryonic progenitors
CD3ε-APC	I45-2C11	BD	embryonic progenitors
NK1.1-APC	PK136	BD	embryonic progenitors
CD19-PECy7 or CD19-PECy5	1D3	BD, eBioscience	embryonic progenitors
B220-PECy7 or B220-PECy5	RA3-6B2	Biolegend	embryonic progenitors
CD45-AlexaFluor700 (AF700)	30-F11	eBioscience	embryonic progenitors
c-Kit-APCeFluor780	2B8	eBioscience	embryonic progenitors
IL7Rα-PE	A7R34	eBioscience	embryonic progenitors
Sca1-PacificBlue (PB) or Sca1-FITC	E13-161.7	Biolegend, BD	embryonic progenitors
Flt3 (CD135)-biotin	A2F10	eBioscience	excluded<E11.5
Streptavidin-Qdot655		Invitrogen	embryonic progenitors
CD115 (Csf1R)-biotin	AFS98	eBioscinece	embryonic progenitors
ThpoR-biotin	AMM2	Kirin	embryonic progenitors
CD41-PECy7	MWrag30	eBioscience	embryonic progenitors
VE-Cadherin-APC	BV13	eBioscience	embryonic progenitors
CD45.2-AF700	104	Biolegend	embryonic progenitors
PIR-A/B-PerCPeFlour710	6C1	eBioscience	embryonic progenitors
CD19-PE	1D3	BD	Rag1-cre, FL and BM
B220-PETexasRed (PETxRd)	RA3-6B2	BD	Rag1-cre, FL sort
CD41-PECy7	MWrag30	eBioscience	Rag1-cre, FL and BM
Gr1-PacificOrange (PO)	RB6-8C5	Invitrogen	Rag1-cre, FL and BM
CD150-APC	TC15-12F12.2	Biolegend	Rag1-cre, FL and BM
Mac1-AlexaFluor700 (AF700)	M1/70	eBioscence	Rag1-cre, FL and BM
Ter119-PECy5.5 or Ter119-PerCPcy5.5	TER119	eBioscence	Rag1-cre, FL and BM
CD45.1-biotin	A20	BD	Rag1-cre, control sample
Streptavidin PETexasRed (PETxRd)		BD	Rag1-cre, control sample
CD4-AlexaFluor700 (AF700)	RM4-5	eBioscience	Rag1-cre, thymus
CD3ε-APC	145-2C11	eBioscience	Rag1-cre, thymus
Gr1-APC	RB6-8C5	eBioscience	Rag1-cre, thymus
F4/80-APC	BM8	Invitrogen	Rag1-cre, thymus
NK1.1-APC	PK136	eBioscience	Rag1-cre, thymus
CD11c-APC	N418	eBioscience	Rag1-cre, thymus
CD19-APC	1D3	BD	Rag1-cre, thymus
B220-APC	RA3-6B2	BD	Rag1-cre, thymus
c-Kit-APC-eF780	2B8	eBioscience	Rag1-cre, thymus
CD25-PerCPCy5.5	PC61	BD	Rag1-cre, thymus
CD8α-PECy7	53-6.7	eBioscience	Rag1-cre, thymus

Flt3-PE	A2F10	BD, Biolegend	Rag1-cre, thymus
CD45-PacificOrange (PO)	30-F11	Invitrogen	Rag1-cre, thymus

Antibody panels used for characterization of bone marrow progenitors

Antibody-conjugate	Clone	Supplier	Progenitor
Flt3-PE or Flt3-biotin	A2F10	BD, Biolegend eBioscience	HSC, LMPP
CD48-APC	HM48-1	Biolegend	HSC, LMPP
CD150-PECy7	TC15-12F12.2	Biolegend	HSC, LMPP
c-Kit-APC-eF780	2B8	eBioscience	HSC, LMPP
Sca1 PacificBlue (PB)	E13-161.7	Biolegend	HSC, LMPP
CD4-PECy5	RM4-5	BD	HSC, LMPP
CD5-PECy5	53-7.3	Biolegend	HSC, LMPP
CD8α-PECy5	53-6.7	Biolegend	HSC, LMPP
Mac1-PECy5	M1/70	Biolegend	HSC, LMPP
B220-PECy5	RA3-6B2	BD	HSC, LMPP
Ter119-PECy5	TER119	Biolegend	HSC, LMPP
Gr1-PECy5	RB6-8C5	Biolegend	HSC, LMPP
IL7Rα-PE	A7R34	eBioscience	HSC, LMPP
CD19-FITC	1D3	BD	proB
CD43-APC	S7	BD	proB
B220-PE	RA3-6B2	eBioscience	proB
c-Kit-APC-eF780	2B8	eBioscience	proB
CD11c-FITC	N418	eBioscience	CLP
Ly6C-FITC	AL-21	BD	CLP
Flt3-PE	A2F10	BD, Biolegend	CLP
B220-PETexasRed (PETxRd)	RA3-6B2	BD	CLP
Ly6D purified	49-H4	BD	CLP
Sca1-PECy7	E13-161.7	Biolegend	CLP
CD3ε-APC	145-2C11	eBioscience	CLP
Gr1-APC	RB6-8C5	eBioscience	CLP
Mac1-APC	M1/70	Biolegend	CLP
Ter119-APC	TER119	eBioscience	CLP
CD19-AF700	1D3	BD	CLP
c-Kit-APC-eF780	2B8	eBioscience	CLP
IL7Rα biotin	A7R34	eBioscience	CLP
Streptavidin-Qdot655		Invitrogen	CLP
Streptavidin-BrilliantViolet605		Biolegend	CLP,HSC, LMPP
Goat anti-rat F(ab')2 IgG (H+L) Tricolor/PECy5		Invitrogen	CLP

Antibodies used for FACS staining of peripheral blood

Antibody-conjugate	Clone	Supplier
CD45.1-PE	A20	BD
CD45.2-AlexaFluor700 (AF700)	104	Biolegend
CD19-PECy7	1D3	BD, eBioscience
CD4-APCeF780	RM4-5	eBioscience
CD8α-APCeF780	53-6.7	eBioscience
Mac1-APC	M1/70	Biolegend
Gr1-PacificOrange (PO)	RB6-8C5	Invitrogen
NK1.1 PacificBlue (PB)	PK136	Biolegend

Viability dyes for FACS

Viability dye	Supplier
TO-PRO-1	Invitrogen
DAPI (4',6-diamidino-2-phenylindole, dihyrochloride	Invitrogen
Propidium Iodide	Invitrogen
7-Aminoactinomycin D (7-AAD)	Sigma

Configurations of FACS instruments

Instrument	Laser wavelength	Laser power	PMTs and filter configurations
BD FACS AriaIIu	Violet 405nm	100 mW	QD655: 660/40: QD605: 610/20; Pacific Blue: 450/50;
	Blue 488nm	100 mW	PerCP: 675/20; FITC: 525/50; SSC: 488/10
	Green 532 nm	150 mW	PECy7: 780/60; PECy5.5: 710/50; PECy5: 685/35; PETxRd: 610/20; PE: 575/26
	Red 640 nm	40 mW	APCeFluor780: 780/60; AlexaFluor700: 730/45; APC: 670/14
BD LSRII	Violet 405nm Blue 488nm	50 mW 100 mW	QD655: 660/40: QD605: 610/20; Pacific Blue: 450/50; FITC: 525/50; SSC: 488/10
	Green 532 nm	150 mW	PECy7: 780/60; PECy5.5: 710/40; PECy5: 685/35; PETxRd: 610/20; PE: 575/25
	Red 640 nm	40 mW	APCeFluor780: 780/60; AlexaFluor700: 730/45; APC: 670/14
BD FACS AriaI	Violet 405nm	50 mW	QD655: 660/40: QD605: 610/20; Pacific Blue: 440/40;
	Blue 488nm	100 mW	PECy7: 780/60; PECy5.5: 710/40; PECy5: 665/30; PETxRd: 605/20; PE: 576/26; FITC: 525/50; SSC: 488/10
	Red 640 nm	40 mW	APCeFluor780: 780/60; AlexaFluor700: 710/40; APC: 670/14
BD LSRII	Violet 405nm	50 mW	QD655: 660/40: QD605: 610/20; Pacific Blue: 440/40;
	Blue 488nm	100 mW	PECy7: 780/60; PECy5.5: 710/40; PECy5: 665/30; PETxRd: 610/20; PE: 576/26; FITC: 525/50; SSC: 488/10
	Red 640 nm	40 mW	APCeFluor780: 780/60; AlexaFluor700: 710/40; APC: 670/14

***In vitro* evaluation of MkE and GM potential and cytokine response**

Evaluation of MkE and GM lineage potentials was performed as previously described with minor modifications (Adolfsson et al., 2005; Luc et al., 2008a; Mansson et al., 2007). In brief, cells from indicated populations were manually plated at a density of 0.5 or 1 cell per well into Terasaki plates with X-vivo15 medium (BioWhittaker^{TM}) supplemented with 1% Penicillin/Streptomycin (PAA), 1% L-glutamine (2mM, PAA), 1% 2-Mercaptoethanol (0.1mM, Sigma-Aldrich) and 10-20% fetal calf serum (FCS, Sigma-Aldrich or HyClone) supplemented with cytokines as specified in the **Table below**. In some experiments X-vivo15 with Gentamycin (Lonza) was used and no Penicillin/Streptomycin was added. For cytokine response studies, single cells were evaluated in X-vivo15 medium in which FCS was replaced with 0.5% detoxified Bovine Serum Albumin (BSA; Sigma-Aldrich)(see also **Table below**). GM as well as Mk and E colonies were evaluated at day 7-10. To determine frequencies of erythroid colonies 2,7-diaminofluorene (DAF; Sigma-Aldrich) staining was used. To investigate granulocyte potential 10-20 progenitor cells were plated in Granulocyte (G) promoting media (with or without mGM-CSF; see **Table below**) and cytospins made at days 3-6. The lineage identity of colonies was evaluated on May-Grünwald (Sigma) and Giemsa (Fluka) stained cytospin slides. Megakaryocyte potential was additionally evaluated with a Megacult collagen-based assay (StemCell Technologies) supplemented with growth factors as specified in the **Table below** and colonies were evaluated after 7 days by acetylthiocholiniodide staining according to manufacturer's instructions (Sigma). In addition, E10.5 and E11.5 FL progenitors were plated in complete methylcellulose (MethoCult GF M3434, Stem Cell Technologies Inc - containing mSCF, mIL-3, hIL-6 and hEPO) and erythroid colonies were evaluated by 2,7-diaminofluorene (DAF; Sigma-Aldrich) staining after 7-10 days (Mansson et al., 2007).

***Rag1-Cre* fate mapping**

Controls for unspecific YFP labelling (cross-over) were made by mixing CD45.1 wild type BM cells with *Rag1-Cre*$^{tg/+}$*R26R*$^{eYFP/+}$ BM or FL cells (expressing CD45.2) and adding an anti-CD45.1 antibody to the staining. The unspecific cross-over was reproducibly found to be up to 1% in the GM, Mk and E lineages. To perform fate mapping of colony forming progenitors, unfractionated E14.5 FL cells (40 000 cells) were plated in MethoCult GF M3434 (containing mSCF, mIL-3, hIL-6 and hEPO) supplemented with hTHPO to promote erythroid colony growth and MethoCult M3134 (supplemented with mIL-3, hFLT3, hG-CSF and mGM-CSF or with mSCF and hG-CSF), to promote GM and G colony formation respectively (see **Table below**). YFP^{+} and YFP^{-} erythroid and GM containing colonies were scored with a fluorescence microscope after 6-9 days. Colonies generated from WT littermates were used as negative controls. The lineage identity of colonies was evaluatedon May-Grünwald and

Giemsa stained cytospin slides. To further confirm that YFP positive cells were myeloid, $Mac1^{+}Gr1^{+}YFP^{+}$ and $Mac1^{+}Gr1^{-}YFP^{+}$ cells (that were also $CD19^{-}B220^{-}Ter119^{-}CD41^{-}CD150^{-}$) were FACS purified and the morphology evaluated on May-Grünwald/Giemsa stained cytospins.

***In vitro* lymphoid potential and combined lineage potential assays**

For evaluation of lymphoid potential, single cells (E11.5 FL) or 4 cells/well (E10.5 FL) were plated onto Op9 or Op9DL1 stroma cells with cytokines (see **Table below**). Cells were picked and analysed by FACS after 12-21 days, and regarded as B cells if they had an $NK1.1^{-}CD19^{+}$ phenotype and as T cells if they had an $NK1.1^{-}CD25^{+}Thy1.2^{hi}$ and/or $NK1.1^{-}CD4^{+}CD8^{+}$ phenotype. In the switch culture system (Mansson et al., 2007) single cells were deposited by a single cell depositor unit directly into wells with Op9 stroma cells. Cultures were transferred from Op9 to Op9DL1 stroma after 5 days of culture and analysed after a total of 11 days. Clones were defined based on the following markers; B cells - $NK1.1^{-}CD19^{+}$; T-cells -$NK1.1^{-}CD19^{-}CD25^{+}Thy1.2^{hi}$ cells and/or $NK1.1^{-}CD4^{+}CD8^{+}$; GM - $NK1.1^{-}CD19^{-}CD25^{-}Thy1.2^{-}Gr1^{+/-}Mac1^{+}$ and NK cells -$NK1.1^{+}CD19^{-}CD25^{-}Thy1.2^{-}$ (see **Table below**).

Cytokines used in in vitro assays

Growth factor	Supplier	Final conc	Assay
mouse stem cell factor (mSCF)	PeproTech, R&D Systems	25-50ng/ml	Terasaki MkE and GM and G
		50ng/ml	Methocult M 3134
		50ng/ml	E potential (Op9)
		25ng/ml	B (Op9), T (Op9DL1) and combined potential
mouse interleukin-3 (mIL-3)	PeproTech, R&D Systems	10-20ng/ml	Terasaki MkE and GM and G
		2ng/ml	Methocult M 3134
		10ng/ml	Megacult
human Flt3 Ligand (hFLT3L)	Immunex	25-50ng/ml	Terasaki MkE and GM and G
		10ng/ml	Methocult M 3134
		50ng/ml	Response assay
		25ng/ml	B (Op9), T (Op9DL1) and combined potential
Human Thrombopoietin (hTHPO)	PeproTech	25-50ng/ml	Terasaki MkE and GM and G
		50ng/ml	Megacult
		50ng/ml	added to MethoCult GF 3434-*Rag1*-cre
		50ng/ml	E potential (Op9)
human Erythropoietin (hEPO)	Recormon, Janssen-Cilag	5U/ml	Terasaki MkE and GM
		5U/ml	E potential (Op9)
human Granulocyte-Colony Stimulating Factor (hG-CSF)	Amgen	25-50ng/ml	Terasaki GM and G
		10ng/ml	Methocult M 3134
mouse Granulocyte Monocyte-Colony Stimulating Factor (mGM-CSF)	PeproTech, Immunex	25-50ng/ml	Terasaki GM
		5ng/ml	Methocult M 3134
human interleukin 6 (hIL-6)	PeproTech	20ng/ml	Megacult
human interleukin 11 (hIL-11)	Genetics Institute Inc	50ng/ml	Megacult
human interleukin 7 (hIL-7)	PeproTech, R&D Systems	50ng/ml	Response assay
		20ng/ml	B (Op9) and combined potential

Antibodies used for FACS staining of in vitro cultures

Antibody-conjugate	Clone	Supplier	Assay
B220-PE or B220-FITC	RA3-6B2	BD, eBioscience	B (Op9) potential
CD19-PECy7	1D3	BD, eBioscience	B (Op9) potential
Gr1-APC	RB6-8C5	eBioscence	B (Op9) potential
Mac1-AlexaFluor700 (AF700)	M1/70	eBioscence	B (Op9) potential
NK1.1 PacificBlue (PB)	PK136	Biolegend	B (Op9) potential
CD45-PacificOrange (PO)	30-F11	Invitrogen	B and T potential
CD25-PE	3C7	BD	T (Op9DL1)/combined potential
CD19-PECy7	1D3	BD, eBioscience	T (Op9DL1)/combined potential
Thy1.2-APC	53-2.1	BD	T (Op9DL1)/combined potential
Mac1-AlexaFluor700 (AF700)	M1/70	eBioscence	T (Op9DL1)/combined potential
NK1.1 PacificBlue (PB)	PK136	Biolegend	T (Op9DL1)/combined potential
Gr1-PECy5	RB6-8C5	eBioscience	combined potential
CD4-PE	H129.19	Biolegend	T (Op9DL1) potential
CD8α-PECy7	53-6.7	eBioscence	T (Op9DL1) potential
Thy1.2-APC	30-H12	Biolegend	T (Op9DL1) potential
CD25-PerCPCy5.5	PC61	BD	T (Op9DL1) potential
NK1.1 PacificBlue (PB)	PK136	Biolegend	T (Op9DL1) potential
CD71-PE	RI7217	Biolegend	E potential (Op9)
CD41-PECy7	MWrag30	eBioscience	E potential (Op9)
TER119 PECy5.5	TER119	eBioscence	E potential (Op9)
Gr1-PacificOrange (PO)	RB6-8C5	Invitrogen	E potential (Op9)
Mac1-AlexaFluor700 (AF700)	M1/70	eBioscence	E potential (Op9)
CD150-APC	TC15-12F12.2	Biolegend	E potential (Op9)

Explant cultures

Pre-circulation dissected YS and PAS whole explants were transferred into individual wells of 24 wells plate or in 8 well μ-Slides (ibidi), while the embryo remnants were used for genotyping. Explants were cultured for 48 hours in OptiMEM with Glutamax (life technologies) supplemented with 1% Penicillin/Streptomycin, 0.1-1% 2-Mercaptoethanol and 10% FCS and whole mount immunostained afterwards or taken for quantitative PCR (see below).

Whole mount immunostaining

Embryos and YS were dissected and fixed in 4% paraformaldehyde solution for 30 minutes at 4°C. Samples were then treated with a permabilizing-blocking solution (0.2% Triton X-100, 2% donkey serum) and incubated overnight with primary antibodies. A second step of incubation with appropriate secondary antibodies was then carried out. The antibodies used are described in the **Table below**. Subsequently, YS were cleared in a 50% solution of glycerol in PBS before being flat-mounted on Superfrost microscope slides. Embryos were processed with a tissue transparency treatment as previously described (Yokomizo et al., 2012) and imaged using a Zeiss 780 confocal system.

Antibodies used for whole mount immunostaining

Antibody-conjugate	Host	Clone	Supplier
Anti-GFP	Rabbit	Polyclonal	Molecular Probes
Anti-CD31	Goat	Polyclonal	R&D Systems
Anti-CD45 APC-Cy7	Rat	30-F11	BD
Anti-Rabbit Alexa 488	Donkey		Molecular Probes
Anti-Goat Alexa 555	Donkey		Molecular Probes
Anti-Rat Alexa 647	Chicken		Molecular Probes

Single cell and quantitative PCR

Multiplex single-cell RT-PCR analysis was performed as previously described (Adolfsson et al., 2005; Mansson et al., 2007). As investigated progenitors were purified based on c-Kit expression, only cells expressing *Kit* were included in the analysis (>90% of total cells). For E11.5 FL populations single cells were deposited by an automated cell deposition unit (ACDU), whereas cells from E9.5 YS were bulk sorted and single cells were micro-manipulated into lysis buffer. Combined lymphoid and GM transcriptional priming was established based on co-expression of relevant genes as previously described (Mansson et al., 2007). Multiplex quantitative real time PCR analysis was performed with the BioMark 48.48 or 96.96 Dynamic Array platform (Fluidigm) and TaqMan Gene Expression Assays (Applied Biosystems) as previously described (Tehranchi et al., 2010).. For quantitative real time PCR analysis of dissected embryonic tissue, cells were dissolved into buffer-RLT with 1% 2-Mercaptoethanol and frozen at −80°C. RNA extraction and DNase treatment was performed with the RNeasy Micro kit (Qiagen). Eluted RNA samples were reverse transcribed using SuperScript II and random hexamers (Invitrogen) according to the manufacturer´s protocol. PCR reactions were performed by mixing 2×TaqMan universal PCR master mix, 20× Assays-on-Demand (primer/MGB-probe mix), RNase-free H_2O and cDNA.

TaqMan primers used for the analysis are shown in the **Table below**. Data were analysed using the ΔCt method; results were normalized to hypoxanthine guanine phosphoribosyltransferase 1 (*Hprt1*) expression and presented as mean expression level relative to *Hprt* ($2^{-\Delta Ct}$). Single cell data were normalized to the mean of *Hprt* and *Gapdh*

and are shown as ΔCt values. Only cells expressing *Hprt, Gapdh* and *Kit,* were included in the analysis.

TaqMan primers used for Dynamic arrays

Assay name	Assay Id
Ccr7	Mm01301785_m1
Ccr9	Mm02528165_s1, Mm02620030_s1
Csf1r	Mm00432689_m1, Mm01266652_m1
Csf2ra (Gmcsfr)	Mm00438331_g1
Csf3r (Gcsfr)	Mm00432735_m1
Klf1 (Eklf)	Mm00516096_m1, Mm04208330_g1
Epor	Mm00438760_m1
Flt3	Mm00439016_m1
Gata1	Mm00484678_m1, Mm01352636_m1
Gapdh	Mm99999915_g1
Hes1	Mm01342805_m1
Hprt	Mm00446968_m1, Mm01545399_m1
Ighm	Mm01718955_g1
Il7r	Mm00434295_m1
Kit	Mm00445212_m1
Lilrb3 (PirB)	Mm01700366_m1
Pax5	Mm00435501_m1
Ptcra	Mm00478363_m1, Mm00478363_m1
Rag2	Mm00501300_m1
sIgh	Custom assay Forward primer: GGACTTTGGGATGGGTTTGGTT Reverse primer: CCCTGGTCCTAGACATCAGAGTAAT Reporter sequence: CCCAGATGAAGGGCTAC

RNA Sequencing

Samples for RNA sequencing were prepared using the SMARTer™ Ultra Low RNA kit for Illumina Sequencing (Clontech) as previously described (Ramskold et al., 2012). Briefly, cDNA libraries were prepared from 73-100 cells were deposited directly into cell lysis buffer followed by 15 cycles of amplification. Amplified cDNA libraries were sheared using Covaris AFA system. NEBNext® DNA Library Prep Reagent Set for Illumina® (New England Biolabs) was used to repair ends after DNA shearing, adenylate 3' ends, ligate genomic adaptors and PCR amplification using Genomic DNA Sample Prep oligos (Illumina). 5-6 samples with different indexes were pooled per lane and adjusted to 2 nM before cluster preparation. Pools were sequenced on HiSeq 2000 (Illumina) generating single–end, 50 bp reads. Reads were aligned using Bowtie (Langmead et al., 2009) against the murine genome assembly (mm9) and against the

murine transcriptome (Refseq and Ensembl, version from 31 Jul 2011 and 16 May 2011, respectively). Gene expression levels for Refseq transcripts were summarized as reads per kilobase of exon model per million mapped reads (RPKM) and read counts using Rpkmforgenes (Ramskold et al., 2012). The RPKM values were used when investigating the expression of specific genes. The non-adjusted read counts for each gene was used for statistical calculation of global differential expression between the specified populations using the DESeq package (version 1.6.1) for R (version 2.14.2) (Anders and Huber, 2010). Genes which were significant at a 10% false discovery rate (calculated using a Benajmini-Hochberg adjusted p-value) were considered differentially expressed between populations. Gene ontology enrichment was assessed using GeneMania (www.genemania.org, annotations performed 6th May 2012) (Warde-Farley et al., 2010). Annotation of genes was performed both using the BioMart tool at www.ensembl.org and available published literature. In addition to validation of gene expression data generated from RNA sequencing analysis by quantitative PCR, the method has been validated for sensitivity, specificity and transcript coverage down to the single cell level (Ramskold et al., 2012).

SUPPLEMENTAL REFERENCES

Anders, S., and Huber, W. (2010). Differential expression analysis for sequence count data. Genome Biol *11*, R106.

Andreu, A.L., Nogales-Gadea, G., Cassandrini, D., Arenas, J., and Bruno, C. (2007). McArdle disease: molecular genetic update. Acta Myol *26*, 53-57.

Angata, K., Chan, D., Thibault, J., and Fukuda, M. (2004). Molecular Dissection of the ST8Sia IV Polysialyltransferase. J Biol Chem *279*, 25883-25890.

Atkinson, S.P., Collin, J., Irina, N., Anyfantis, G., Kyung, B.K., Lako, M., and Armstrong, L. (2012). A putative role for the immunoproteasome in the maintenance of pluripotency in human embryonic stem cells. Stem Cells *30*, 1373-1384.

Bee, T., Swiers, G., Muroi, S., Pozner, A., Nottingham, W., Santos, A.C., Li, P.S., Taniuchi, I., and de Bruijn, M.F. (2010). Nonredundant roles for Runx1 alternative promoters reflect their activity at discrete stages of developmental hematopoiesis. Blood *115*, 3042-3050.

Benarafa, C., LeCuyer, T.E., Baumann, M., Stolley, J.M., Cremona, T.P., and Remold-O'Donnell, E. (2011). SerpinB1 protects the mature neutrophil reserve in the bone marrow. J Leukoc Biol *90*, 21-29.

Benz, C., Martins, V.C., Radtke, F., and Bleul, C.C. (2008). The stream of precursors that colonizes the thymus proceeds selectively through the early T lineage precursor stage of T cell development. J Exp Med *205*, 1187-1199.

Bermudez, O., Pages, G., and Gimond, C. (2010). The dual-specificity MAP kinase phosphatases: critical roles in development and cancer. American journal of physiology Cell physiology *299*, C189-202.

Borrego, F., Masilamani, M., Kabat, J., Sanni, T.B., and Coligan, J.E. (2005). The cell biology of the human natural killer cell CD94/NKG2A inhibitory receptor. Mol Immunol *42*, 485-488.

Brinkman-Van der Linden, E.C., Angata, T., Reynolds, S.A., Powell, L.D., Hedrick, S.M., and Varki, A. (2003). CD33/Siglec-3 binding specificity, expression pattern, and consequences of gene deletion in mice. Molecular and cellular biology *23*, 4199-4206.

Budanov, A.V. (2011). Stress-responsive sestrins link p53 with redox regulation and mammalian target of rapamycin signaling. Antioxid Redox Signal *15*, 1679-1690.

Carabana, J., Watanabe, A., Hao, B., and Krangel, M.S. (2011). A barrier-type insulator forms a boundary between active and inactive chromatin at the murine TCRbeta locus. J Immunol *186*, 3556-3562.

Chae, Y.C., Lee, S., Heo, K., Ha, S.H., Jung, Y., Kim, J.H., Ihara, Y., Suh, P.G., and Ryu, S.H. (2009). Collapsin response mediator protein-2 regulates neurite formation by modulating tubulin GTPase activity. Cell Signal *21*, 1818-1826.

Chiles, T.C. (2004). Regulation and function of cyclin D2 in B lymphocyte subsets. J Immunol *173*, 2901-2907.

Clement, L.T. (1992). Isoforms of the CD45 common leukocyte antigen family: markers for human T-cell differentiation. J Clin Immunol *12*, 1-10.

Datta, M., Choudhury, A., Lahiri, A., and Bhattacharyya, N.P. (2011). Genome wide gene expression regulation by HIP1 Protein Interactor, HIPPI: prediction and validation. BMC Genomics *12*, 463.

de Bruijn, M.F., and Speck, N.A. (2004). Core-binding factors in hematopoiesis and immune function. Oncogene *23*, 4238-4248.

Denoeud, J., and Moser, M. (2011). Role of CD27/CD70 pathway of activation in immunity and tolerance. J Leukoc Biol *89*, 195-203.

Dittmer, J. (2003). The biology of the Ets1 proto-oncogene. Mol Cancer *2*, 29.

Ea, C.K., Sun, L., Inoue, J., and Chen, Z.J. (2004). TIFA activates IkappaB kinase (IKK) by promoting oligomerization and ubiquitination of TRAF6. Proc Natl Acad Sci U S A *101*, 15318-15323.

El-Benna, J., Dang, P.M., and Perianin, A. (2010). Peptide-based inhibitors of the phagocyte NADPH oxidase. Biochem Pharmacol *80*, 778-785.

Everitt, A.R., Clare, S., Pertel, T., John, S.P., Wash, R.S., Smith, S.E., Chin, C.R., Feeley, E.M., Sims, J.S., Adams, D.J.*, et al.* (2012). IFITM3 restricts the morbidity and mortality associated with influenza. Nature *484*, 519-523.

Faralli, H., Martin, E., Coré, N., Liu, Q.C., Filippi, P., Dilworth, F.J., Caubit, X., and Fasano, L. (2011). Teashirt-3, a novel regulator of muscle differentiation, associates with BRG1-associated factor 57 (BAF57) to inhibit myogenin gene expression. J Biol Chem *286*, 23498-23510.

Flach, H., Rosenbaum, M., Duchniewicz, M., Kim, S., Zhang, S.L., Cahalan, M.D., Mittler, G., and Grosschedl, R. (2010). Mzb1 protein regulates calcium homeostasis, antibody secretion, and integrin activation in innate-like B cells. Immunity *33*, 723-735.

Fuller, D.M., and Zhang, W. (2009). Regulation of lymphocyte development and activation by the LAT family of adapter proteins. Immunol Rev *232*, 72-83.

Gariglio, M., Mondini, M., De Andrea, M., and Landolfo, S. (2011). The multifaceted interferon-inducible p200 family proteins: from cell biology to human pathology. J Interferon Cytokine Res *31*, 159-172.

Gorczynski, R.M., Kai, Y., and Miyake, K. (2006). MD1 expression regulates development of regulatory T cells. J Immunol *177*, 1078-1084.

Harzenetter, M.D., Keller, U., Beer, S., Riedl, C., Peschel, C., and Holzmann, B. (2002). Regulation and function of the CGRP receptor complex in human granulopoiesis. Exp Hematol *30*, 306-312.

Huber, C., Martensson, A., Bokoch, G.M., Nemazee, D., and Gavin, A.L. (2008). FGD2, a CDC42-specific exchange factor expressed by antigen-presenting cells, localizes to early endosomes and active membrane ruffles. J Biol Chem *283*, 34002-34012.

Jongstra-Bilen, J., and Jongstra, J. (2006). Leukocyte-specific protein 1 (LSP1): a regulator of leukocyte emigration in inflammation. Immunol Res *35*, 65-74.

Kallies, A. (2008). Distinct regulation of effector and memory T-cell differentiation. Immunol Cell Biol *86*, 325-332.

Kee, A.J., and Hardeman, E.C. (2008). Tropomyosins in skeletal muscle diseases. Adv Exp Med Biol *644*, 143-157.

Kinoshita, M., Nakamura, T., Ihara, M., Haraguchi, T., Hiraoka, Y., Tashiro, K., and Noda, M. (2001). Identification of human endomucin-1 and -2 as membrane-bound O-sialoglycoproteins with anti-adhesive activity. FEBS Lett *499*, 121-126.

Kusuhara, H., and Sugiyama, Y. (2007). ATP-binding cassette, subfamily G (ABCG family). Pflugers Arch *453*, 735-744.

Kuwata, N., Igarashi, H., Ohmura, T., Aizawa, S., and Sakaguchi, N. (1999). Cutting edge: absence of expression of RAG1 in peritoneal B-1 cells detected by knocking into RAG1 locus with green fluorescent protein gene. J Immunol *163*, 6355-6359.

Langmead, B., Trapnell, C., Pop, M., and Salzberg, S.L. (2009). Ultrafast and memory-efficient alignment of short DNA sequences to the human genome. Genome Biol *10*, R25.

Lee, B.C., Cheng, T., Adams, G.B., Attar, E.C., Miura, N., Lee, S.B., Saito, Y., Olszak, I., Dombkowski, D., Olson, D.P.*, et al.* (2003). P2Y-like receptor, GPR105 (P2Y14), identifies and mediates chemotaxis of bone-marrow hematopoietic stem cells. Genes Dev *17*, 1592-1604.

Lu, Q. (2010). Delta-Catenin dysregulation in cancer: interactions with E-cadherin and beyond. J Pathol *222*, 119-123.

Magdaleno, S., Northcutt, G., Curran, T., and Kurschner, C. (2002). mPPP1R16B is a novel mouse protein phosphatase 1 targeting subunit whose mRNA is located in cell bodies and dendrites of neurons in four distinct regions of the brain. Brain Res Gene Expr Patterns *1*, 143-149.

Maguire, J., Santoro, T., Jensen, P., Siebenlist, U., Yewdell, J., and Kelly, K. (1994). Gem: an induced, immediate early protein belonging to the Ras family. Science *265*, 241-244.

McCormack, M.P., Forster, A., Drynan, L., Pannell, R., and Rabbitts, T.H. (2003). The LMO2 T-cell oncogene is activated via chromosomal translocations or retroviral insertion during gene therapy but has no mandatory role in normal T-cell development. Molecular and cellular biology *23*, 9003-9013.

Meester-Smoor, M.A., Janssen, M.J., Grosveld, G.C., de Klein, A., van IJcken, W.F., Douben, H., and Zwarthoff, E.C. (2008). MN1 affects expression of genes involved in hematopoiesis and can enhance as well as inhibit RAR/RXR-induced gene expression. Carcinogenesis *29*, 2025-2034.

Moratz, C., Kang, V.H., Druey, K.M., Shi, C.S., Scheschonka, A., Murphy, P.M., Kozasa, T., and Kehrl, J.H. (2000). Regulator of G protein signaling 1 (RGS1) markedly impairs Gi alpha signaling responses of B lymphocytes. J Immunol *164*, 1829-1838.

Nakamura, M., Kitaura, J., Enomoto, Y., Lu, Y., Nishimura, K., Isobe, M., Ozaki, K., Komeno, Y., Nakahara, F., Oki, T.*, et al.* (2012). Transforming growth factor-beta-stimulated clone-22 is a negative-feedback regulator of Ras / Raf signaling: Implications for tumorigenesis. Cancer Sci *103*, 26-33.

Nitta, T., and Takahama, Y. (2007). The lymphocyte guard-IANs: regulation of lymphocyte survival by IAN/GIMAP family proteins. Trends Immunol *28*, 58-65.

Ohnishi, K., Melchers, F., and Shimizu, T. (2005). Lymphocyte-expressed BILL-cadherin/cadherin-17 contributes to the development of B cells at two stages. Eur J Immunol *35*, 957-963.

Ong, O.C., Hu, K., Rong, H., Lee, R.H., and Fung, B.K. (1997). Gene structure and chromosome localization of the G gamma c subunit of human cone G-protein (GNGT2). Genomics *44*, 101-109.

Onozawa, Y., Komai, T., and Oda, T. (2011). Activation of T cell death-associated gene 8 attenuates inflammation by negatively regulating the function of inflammatory cells. Eur J Pharmacol *654*, 315-319.

Painter, M.W., Davis, S., Hardy, R.R., Mathis, D., and Benoist, C. (2011). Transcriptomes of the B and T lineages compared by multiplatform microarray profiling. J Immunol *186*, 3047-3057.

Perng, M.D., and Quinlan, R.A. (2005). Seeing is believing! The optical properties of the eye lens are dependent upon a functional intermediate filament cytoskeleton. Exp Cell Res *305*, 1-9.

Pyz, E., Huysamen, C., Marshall, A.S., Gordon, S., Taylor, P.R., and Brown, G.D. (2008). Characterisation of murine MICL (CLEC12A) and evidence for an endogenous ligand. Eur J Immunol *38*, 1157-1163.

Reese, B.E., Krissinger, D., Yun, J.K., and Billingsley, M.L. (2006). Elucidation of stannin function using microarray analysis: implications for cell cycle control. Gene Expr *13*, 41-52.

Rombouts, K., Mello, T., Liotta, F., Galli, A., Caligiuri, A., Annunziato, F., and Pinzani, M. (2012). MARCKS actin-binding capacity mediates actin filament assembly during mitosis in human hepatic stellate cells. American journal of physiology Cell physiology *303*, C357-367.

Rosnet, O., Buhring, H.J., deLapeyriere, O., Beslu, N., Lavagna, C., Marchetto, S., Rappold, I., Drexler, H.G., Birg, F., Rottapel, R.*, et al.* (1996). Expression and signal transduction of the FLT3 tyrosine kinase receptor. Acta Haematol *95*, 218-223.

Rossi, L., Manfredini, R., Bertolini, F., Ferrari, D., Fogli, M., Zini, R., Salati, S., Salvestrini, V., Gulinelli, S., Adinolfi, E.*, et al.* (2007). The extracellular nucleotide UTP is a potent inducer of hematopoietic stem cell migration. Blood *109*, 533-542.

Rothenberg, E.V. (2011). T cell lineage commitment: identity and renunciation. J Immunol *186*, 6649-6655.

Schatz, D.G., and Ji, Y. (2011). Recombination centres and the orchestration of V(D)J recombination. Nat Rev Immunol *11*, 251-263.

Schauer-Vukasinovic, V., Bur, D., Kitas, E., Schlatter, D., Rosse, G., Lahm, H.W., and Giller, T. (2000). Purification and characterization of active recombinant human napsin A. Eur J Biochem *267*, 2573-2580.

Silacci, P., Mazzolai, L., Gauci, C., Stergiopulos, N., Yin, H.L., and Hayoz, D. (2004). Gelsolin superfamily proteins: key regulators of cellular functions. Cell Mol Life Sci *61*, 2614-2623.

Sitkovsky, M., Lukashev, D., Deaglio, S., Dwyer, K., Robson, S.C., and Ohta, A. (2008). Adenosine A2A receptor antagonists: blockade of adenosinergic effects and T regulatory cells. Br J Pharmacol *153 Suppl 1*, S457-464.

Sitnicka, E., Buza-Vidas, N., Ahlenius, H., Cilio, C.M., Gekas, C., Nygren, J.M., Mansson, R., Cheng, M., Jensen, C.T., Svensson, M.*, et al.* (2007). Critical role of FLT3 ligand in IL-7 receptor independent T lymphopoiesis and regulation of lymphoid-primed multipotent progenitors. Blood *110*, 2955-2964.

Srinivas, S., Watanabe, T., Lin, C.S., William, C.M., Tanabe, Y., Jessell, T.M., and Costantini, F. (2001). Cre reporter strains produced by targeted insertion of EYFP and ECFP into the ROSA26 locus. BMC Dev Biol *1*, 4.

Swart, G.W. (2002). Activated leukocyte cell adhesion molecule (CD166/ALCAM): developmental and mechanistic aspects of cell clustering and cell migration. Eur J Cell Biol *81*, 313-321.

Szostecki, C., Guldner, H.H., Netter, H.J., and Will, H. (1990). Isolation and characterization of cDNA encoding a human nuclear antigen predominantly recognized by autoantibodies from patients with primary biliary cirrhosis. J Immunol *145*, 4338-4347.

Tanaka, S.S., Yamaguchi, Y.L., Tsoi, B., Lickert, H., and Tam, P.P. (2005). IFITM/Mil/fragilis family proteins IFITM1 and IFITM3 play distinct roles in mouse primordial germ cell homing and repulsion. Dev Cell *9*, 745-756.

Tehranchi, R., Woll, P.S., Anderson, K., Buza-Vidas, N., Mizukami, T., Mead, A.J., Astrand-Grundstrom, I., Strombeck, B., Horvat, A., Ferry, H.*, et al.* (2010). Persistent malignant stem cells in del(5q) myelodysplasia in remission. The New England journal of medicine *363*, 1025-1037.

Tran, D.Q., Andersson, J., Hardwick, D., Bebris, L., Illei, G.G., and Shevach, E.M. (2009). Selective expression of latency-associated peptide (LAP) and IL-1 receptor type I/II (CD121a/CD121b) on activated human FOXP3+ regulatory T cells allows for their purification from expansion cultures. Blood *113*, 5125-5133.

van de Weerdt, B.C., and Medema, R.H. (2006). Polo-like kinases: a team in control of the division. Cell Cycle *5*, 853-864.

Wang, M., Windgassen, D., and Papoutsakis, E.T. (2008). Comparative analysis of transcriptional profiling of CD3+, CD4+ and CD8+ T cells identifies novel immune response players in T-cell activation. BMC Genomics *9*, 225.

Warde-Farley, D., Donaldson, S.L., Comes, O., Zuberi, K., Badrawi, R., Chao, P., Franz, M., Grouios, C., Kazi, F., Lopes, C.T.*, et al.* (2010). The GeneMANIA prediction server: biological network integration for gene prioritization and predicting gene function. Nucleic Acids Res *38*, W214-220.

Verstrepen, L., Carpentier, I., Verhelst, K., and Beyaert, R. (2009). ABINs: A20 binding inhibitors of NF-kappa B and apoptosis signaling. Biochem Pharmacol *78*, 105-114.

West, K.L., Ito, Y., Birger, Y., Postnikov, Y., Shirakawa, H., and Bustin, M. (2001). HMGN3a and HMGN3b, two protein isoforms with a tissue-specific expression pattern, expand the cellular repertoire of nucleosome-binding proteins. J Biol Chem *276*, 25959-25969.

Westermark, U.K., Wilhelm, M., Frenzel, A., and Henriksson, M.A. (2011). The MYCN oncogene and differentiation in neuroblastoma. Semin Cancer Biol *21*, 256-266.

Yeung, B.H., Law, A.Y., and Wong, C.K. (2012). Evolution and roles of stanniocalcin. Molecular and cellular endocrinology *349*, 272-280.

Yokomizo, T., Yamada-Inagawa, T., Yzaguirre, A.D., Chen, M.J., Speck, N.A., and Dzierzak, E. (2012). Whole-mount three-dimensional imaging of internally localized immunostained cells within mouse embryos. Nat Protoc *7*, 421-431.

Yoshikawa, K., Seto, M., Ueda, R., Obata, Y., Fukatsu, H., Segawa, A., and Takahashi, T. (1993). Isolation and characterization of mouse CD7 cDNA. Immunogenetics *37*, 114-119.